Anonymous Referee #1

Received and published: 30 September 2019

We are very grateful for the referee's critical comments and suggestions. The followings are our point-by-point responses to the comments. Our responses start with "R:".

General comments

The authors report the development of a two-sphere integration spectrophotometer for quantitative measurement of the mass concentration of ambient BC (black carbon) and BC in the snow. As BC is a major light-absorbing aerosol, which will accelerate the snow melt after its deposition onto the surface of snow or ice, thus plays a key role in regional and global climate change. The reported instrument provides an important and useful method for measuring BC in snow. By using the developed instrument, the authors investigated the spatial distribution of BC light absorption in surface snow across northern China during Jan. to Feb. 2014. This section is interesting, which may provide a better constrain of BC simulation in the earth system. I have the following comments to improve the manuscript.

Specific comments

1. Abstract, line 41 and line 42: BC absorption contributed 68.5%-95.9% of total light absorption in the atmosphere and 52.3%-93.3% in seasonal snow over northern China. In my experience, the values for atmosphere air are a bit too high. The wavelength needs to be specified here. Or are they mass concentration contribution?

   Response: Sorry for the misleading. We agreed with the reviewer that the wavelength should be given. In previous version, the absorption contribution of BC to total light absorption was at a wavelength of 600 nm. Compared with previous studies, we have decided to update all of the datasets in this study at the most common wavelength of 550 nm. For this issue, the absorption contribution of BC to total light absorption at 550 nm was lower than that of 600 nm in the revised manuscript. The result is also consistent with the previous study by Wang et al. (2013, their Figure 11).

References:

Wang, X., Doherty, S.J., and Huang, J.P.: Black carbon and other light-absorbing impurities in snow across Northern China, J. Geophys. Res.-Atmos., 118, 1471-1492, doi: 10.1029/2012JD018291, 2013.

2. Page 4, line 101, what is the reason that causes 60% error for snow measurement with SP2 method? More discussion will better show the clear advantage of the developed instrument in this paper over the current available methods. Also in line 106, "biases remain", what are the biases sources? I suggest to give a table to list the uncertainties of each instrument for both ambient and snow measurement.

Response: There are two major issues in leading the large uncertainty. Based on the investigation by Schwarz et al. (2012), the relative transmission efficiencies of polystyrene latex sphere concentration standards (PSLs) in liquid to the SP2 after aerosolization remarkably reduce to 20% due to larger diameter of BC particles (> 500 nm, their Fig. 1). Therefore, the larger diameter of BC (>500 nm) is hardly captured by SP2 instrument with a Collison-type nebulizer. Moreover, the mixing status of BC in snow is more complicated than the standard fullerene soot in the laboratory and the typical BC in the atmosphere. As a summary, they found that the SP2 instrument can be used to measure BC mass concentration in snow with substantially larger uncertainty (60 %) than for atmospheric sampling (<30 %).

References:

Schwarz, J. P., Doherty, S. J., Li, F., Ruggiero, S. T., Tanner, C. E., Perring, A. E., Gao, R. S., and Fahey, D. W.: Assessing Single Particle Soot Photometer and Integrating Sphere/Integrating Sandwich Spectrophotometer measurement techniques for quantifying black carbon concentration in snow, Atmos. Meas. Tech., 5, 2581-2592, 10.5194/amt-5-2581-2012, 2012.

3. Page 5, line 132, is there possible for the loss of light absorption organic aerosol?

Response: We agreed with the reviewer that there is possible to lose the light absorption due to organic carbon. Owing to BC in snow is often hydrophobic, long time melting could lose more BC to the container walls instead of collected on the filter (Ogren et al., 1983). In order to minimize the loss of BC and OC mass, we quickly melted the snow samples in a microwave within a very short time.

Therefore, the loss of insoluble organic aerosols is very limited, and can be neglectable. At present, this method is widely performed for snow melting procedure. (Doherty et al., 2010,2014; Wang et al.,2013).

References:

Ogren, J. A., Charlson, R. J., and Groblicki, P. J.: Determination of elemental carbon in rainwater, Anal. Chem., 55, 1569–1572,1983.

Doherty, S.J., Warren, S.G., Grenfell, T.C., Clarke, A.D., and Brandt, R.E.: Light-absorbing impurities in Arctic snow, Atmos. Chem. Phys., 10, 11647-11680, doi: 10.5194/acp-10-11647-2010, 2010.

Doherty, S.J., Dang, C., Hegg, D.A., Zhang, R.D., and Warren, S.G.: Black carbon and other light-absorbing particles in snow of central North America, J. Geophys. Res.-Atmos., 119, 12807-12831, doi: 10.1002/2014JD022350, 2014.

Wang, X., Doherty, S.J., and Huang, J.P.: Black carbon and other light-absorbing impurities in snow across Northern China, J. Geophys. Res.-Atmos., 118, 1471-1492, doi: 10.1029/2012JD018291, 2013.

4. Page 7, the spectrum information and an example for the data processing for this part are encouraged to be shown in the supporting information. The wavelength should be specified? Did the authors make an average over the selected range?

   Response: We feel sorry for the misleading. We have carefully unified all of the relative spectrum at a given wavelength of 550 nm and replotted the relative Figures in the revised manuscript.

5. Page 9, line 234, there is a typo. Figure 2 should be Figure 3. How to determine the filter loading?

   Response: Corrected.

6. Page 10, Fig. 4 was lost in the text.

   Response: We have corrected this mistake and added the relative description of Figure 4 in Page 11, Line 303.

7. the results got from TSI method were smaller than that with the two-step method for the snow samples over northeast China (Fig. 6), but the results for Lanzhou

were the opposite (Fig. 7). Some more discussion is encouraged to explain the underestimated and overestimated of these two methods?

Response: We feel sorry for the misleading. However, there seems no discrepancy for Figure 6 and Figure 7. As seen in Figure 5, it clearly shows that the loss of BC is in the range of 12-20% due to 1-μm quartz fiber filters. Therefore, if we scaled the BC mass in the atmosphere as 120% based on the thermal optical method, the results of BC concentration in the atmosphere should be much similar as Figure 6. Therefore, we concluded that the thermal–optical method underestimates BC concentrations by 35%–45% than that measured by TSI technique.

8. Page 12, line 322, is this method related to size distribution?

   Response: This technique on estimating BC light absorption is only based on the integrated light absorption in the wavelength of 400-750 nm due to all insoluble LAPs on the Nuclepore filters. Therefore, this method is nothing relevant with the snow grain size. However, there is still a need to provide the information of the snow grain size during the snow field campaign, which is the key parameter in determining the snow albedo, and pretty useful in validating the radiative transfer models.

9. Page 34, Fig. 3, the Y axis should be S/S0, not –ln(S/S0). The authors gave the fit equation in the figure: y = a*exp(-b*x)+c.

   Response: We have corrected this mistake, and replotted Fig. 3. Therefore, the Y axis is still given as the relative attenuation (Atn), Atn = $-\ln[S/S_0]$.

Anonymous Referee #2

Received and published: 08 October 2019

We are very grateful for the referee's critical comments and suggestions. The followings are our point-by-point responses to the comments. Our responses start with "R:".

The paper describes a new methodology for quantifying black carbon concentration in the atmosphere and seasonal snow. The article is appropriate for the AMT journal. The authors have described the methodology in detail and have presented comparison with thermal-optical method. Real data from field has also been presented. I recommend that the article may be published in the AMT journal. My specific comments are:

1. Line 260: What are the factors contributing to the uncertainty? How they are estimated. A little bit more explanation is desired.

   Response: As Schwarz et al. (2012) illustrated, the total uncertainty associated with the filter-based ISSW technique on BC concentration determination for ambient snow has previously been estimated as 40 %, which is the sum, in quadrature, of 11% for instrumental uncertainty, 15% for undercatch uncertainty (loss of insoluble light-absorbing impurities), 17% for BC MAC uncertainty, and 30% for uncertainty in the AAE of non-BC material (Doherty et al., 2010; Grenfell et al., 2011). The relative description has been added in introduction section in Page 4, Line 99-105.

2. Line 213, line 231-234, and 278: Mass absorption cross-sections (MAC) at 550 nm 525 nm were assumed. Any reference related to this that may be cited? How broad of the spectrum was averaged for computation using MAC at these wavelengths? Could the uncertainty due to the error in the assumption of MAC be quantified?

   Response: Generally, the MAC has been widely reviewed as ~7.5 m^2 g^{-1} at _=550 nm by previous studies (Clarke et al., 2004; Bond and Bergstrom, 2006). However, to estimate the BC radiative forcing in snow, what we really need to know is not the mass of BC but rather its effect on snow albedo, which is closely related to its absorptance on the filter. As a result, Doherty et al. (2010) reported that the MAC should be used with β abs =6.0 m^2 g^{-1} at λ = 550 nm or else scaled appropriately in

radiation models. In this study, the value of mass absorption coefficient is given as 6.22 m^2 g^{-1} at 550 nm, which is consistent with recent studies by Wang et al. (2013). As illustrated by Schwarz et al. (2012), the total uncertainty associated with the filter-based ISSW technique on BC concentration determination for ambient snow has previously been estimated as 17% for BC MAC uncertainty.

Reference

Bond, T. C. and Bergstrom, R. W.: Light absorption by carbonaceous particles: an investigative review, Aerosol Sci. Tech., 40, 27–67, 2006.

Clarke, A. D., Shinozuka, Y., Kapustin, V. N., Howell, S., Huebert, B., Doherty, S., Anderson, T., Covert, D., Anderson, J., Hua, X., Moore II, K. G., McNaughton, C., Carmichael, G., and Weber, R.: Size distributions and mixtures of dust and black carbon aerosol in Asian outflow: Physiochemistry and optical properties, J. Geophys. Res., 109, D15S09, doi:10.1029/2003JD004378, 2004.

Doherty, S.J., Warren, S.G., Grenfell, T.C., Clarke, A.D., and Brandt, R.E.: Light-absorbing impurities in Arctic snow, Atmos. Chem. Phys., 10, 11647-11680, doi: 10.5194/acp-10-11647-2010, 2010.

Doherty, S. J., Dang, C., Hegg, D. A., Zhang, R. D., and Warren, S. G.: Black carbon and other light-absorbing particles in snow of central North America, J. Geophys. Res.-Atmos., 119, 12807-12831, doi: 10.1002/2014jd022350, 2014.

Wang, X., Doherty, S.J., and Huang, J.P.: Black carbon and other light-absorbing impurities in snow across Northern China, J. Geophys. Res.-Atmos., 118, 1471-1492, doi: 10.1029/2012JD018291, 2013.

Schwarz, J. P., Doherty, S. J., Li, F., Ruggiero, S. T., Tanner, C. E., Perring, A. E., Gao, R. S., and Fahey, D. W.: Assessing Single Particle Soot Photometer and Integrating Sphere/Integrating Sandwich Spectrophotometer measurement techniques for quantifying black carbon concentration in snow, Atmos. Meas. Tech., 5, 2581-2592, 10.5194/amt-5-2581-2012, 2012.

3. Figure 2 depicts the schematic of the developed TSI instrument. It would be beneficial to list out the components used in the instrument. For example, what was the light source, what wavelength range etc. Similarly on the detector side, and if any optical filters were used.

Response: Figure 2 has been updated based on the reviewer's suggestion, and all major components used to design this instrument are listed.

4. Is broadband attenuation measurement possible with this instrument? If so could this be useful for further speciation based on broad absorption properties?
   Response: This instrument is designed to measure the total light absorption due to the insoluble light-absorbing impurities at the visible wavelengths. Right now, we have confidence that this instrument could be updated to capture the fluorescence signals in the ultraviolet (UV) wavelengths by changing a strong power UV light sources. However, we have no idea if the similar instrument is effective on the broadband attenuation measurement.

5. Filter loading is a common problem in similar instruments. Some details on how this was dealt with would be beneficial.
   Response: The filter-based technique on measuring light-absorbing aerosols in the atmosphere and snow/ice is designed since 1965, and has been developed for half century. The accuracy on measuring BC based on this technique has been enhanced significantly. However, due to the complex of the BC mixing status in the atmosphere and snow/ice, there are still visible uncertainties. According to the previous study by Schwarz et al. (2012), the total uncertainty associated with the filter-based ISSW technique on BC concentration determination for ambient snow has previously been estimated as 40 %, which is the sum, in quadrature, of 11% for instrumental uncertainty, 15% for undercatch uncertainty (loss of insoluble light-absorbing impurities), 17% for BC MAC uncertainty, and 30% for uncertainty in the AAE of non-BC material (Doherty et al., 2010; Grenfell et al., 2011). Therefore, the major novelty of this updated technique is to minimize the light scattering due to the insoluble impurities based on two integrating sphere configurations. Finally, we also assess the loss of the BC concentration using Nuclepore filters with 0.4-μm and 0.2-μm pores during the filtration process.

Reference

Doherty, S.J., Warren, S.G., Grenfell, T.C., Clarke, A.D., and Brandt, R.E.: Light-absorbing impurities in Arctic snow, Atmos. Chem. Phys., 10, 11647-11680, doi: 10.5194/acp-10-11647-2010, 2010.

Grenfell, T. C., Doherty, S. J., Clarke, A. D., and Warren, S. G.: Light absorption from particulate impurities in snow and ice determined by spectrophotometric analysis of filters, Appl. Opt., 50, 2037-2048, 2011.

Schwarz, J. P., Doherty, S. J., Li, F., Ruggiero, S. T., Tanner, C. E., Perring, A. E., Gao, R. S., and Fahey, D. W.: Assessing Single Particle Soot Photometer and Integrating Sphere/Integrating Sandwich Spectrophotometer measurement techniques for quantifying black carbon concentration in snow, Atmos. Meas. Tech., 5, 2581-2592, 10.5194/amt-5-2581-2012, 2012.

Development of an improved two-sphere integration technique for quantifying black carbon concentrations in the atmosphere and seasonal snow

Xin Wang [1, 2], **Xueying Zhang** [3] and Wenjing Di [1]

[1] Key Laboratory for Semi-Arid Climate Change of the Ministry of Education, Lanzhou University, Lanzhou 730000, Gansu, China

[2] Institute of Surface-Earth System Science, Tianjin University, Tianjin 300072

[3] Jilin Weather Modification Office, Changchun 132000, Jilin, China

Correspondence to: Xin Wang (Tel: +86 931 8915892)

E-mail address: wxin@lzu.edu.cn (X. Wang)

Submitted on August 2019

删除的内容: and **Wenjing Di**

删除的内容: [1]

Abstract. An improved two-sphere integration (TSI) technique has been developed to quantify black carbon (BC) concentrations in the atmosphere and seasonal snow. The major advantage of this system is that it combines two distinct integrated-spheres to reduce the scattering effect due to light-absorbing particles, and thus provides accurate determinations of total light absorption from BC collected on Nuclepore filters. The TSI technique can be calibrated using a series of 15 filter samples of standard fullerene soot. This technique quantifies the mass of BC by separating the spectrally resolved total light absorption into BC and non-BC fractions. To assess the accuracy of the improved system, an empirical procedure for measuring BC concentrations by a two-step thermal–optical method is also applied. Laboratory results indicate that BC concentrations determined using the TSI technique and theoretical calculations are well correlated (R^2=0.99), whereas the thermal–optical method underestimates BC concentrations by 35%–45% than that measured by TSI technique. Assessments of the two methods for atmospheric and snow samples revealed excellent agreement, with least-squares regression lines with slopes of 1.72 (r^2 = 0.67) and 0.84 (r^2 = 0.93), respectively. However, the TSI technique is more accurate in quantifications of BC concentrations in both the atmosphere and seasonal snow, with an overall lower uncertainty. Using the improved TSI technique, we find that light absorption at a wavelength of 550 nm due to BC plays a dominant role, relative to non-BC light absorption, in both the atmosphere (62.76%–91.84% of total light absorption) and seasonal snow (43.11%–88.56%) over northern China.

ARTICLE INFO

Keywords:

Black carbon

Elemental carbon

Light absorption

Two-sphere integration technique

Thermal–optical method

带格式的: 上标

删除的内容: 68.5

删除的内容: 95.9

删除的内容: 52.3

删除的内容: 93.3

带格式的: 不对齐到网格

1 Introduction

Black carbon (BC) has long been recognized as the major light-absorbing particles (LAPs) in both natural and anthropogenic emissions (Slater et al., 2002; Koch et al., 2009; Zhang et al., 2009; Pan et al., 2010; McMeeking et al., 2011; Pavese et al., 2012; Bond et al., 2013; IPCC, 2013). BC can impact the regional and global climate in several ways, including via the direct effects of scattering and absorbing visible solar radiation (Jacobson, 2001b; Menon et al., 2002; Hansen et al., 2005; Ramanathan and Carmichael, 2008), the semi-direct effects of changing the temperature structure and relative humidity of the atmosphere by absorbing solar short-wave radiation (Weiss et al., 2012), and indirect effects on cloud formation and lifetime (Chuang et al., 2002; Baumgardner et al., 2004; Rosenfeld et al., 2008). Once deposited onto snow or ice surfaces, BC absorbs more solar radiation than pure snow or ice and reduces the snow albedo, thus accelerating snow melt (Xu et al., 2009a; Flanner et al., 2012; Hadley and Kirchstetter, 2012; Carmagnola et al., 2013; Qian et al., 2014; Zhao et al., 2014).

Optically classified BC is also often referred to as elemental carbon (EC), which is typically thermally detected. The distinction between BC and EC has been debated since the 1980s (Heintzenberg, 1989; Horvath, 1993a; Andreae and Gelencser, 2006; Moosmuller et al., 2009). Given that BC and EC are both soot particles with diameters of <1 μm, these terms have often been used interchangeably (Chow et al., 2001, 2004; Ming et al., 2009; Thevenon et al., 2009; Lim et al., 2014). BC is generally regarded as ideal light-absorbing particles of carbon, and is typically measured using optical attenuation methods (Clarke et al., 1987; Grenfell et al., 2011; Hansen et al., 1984; Ogren and Charlson, 1983). The term 'EC' is often used interchangeably with 'BC' when referring to optical absorption measurements (Clarke et al., 1987; Grenfell et al., 2011), and is only uniquely identified by thermal–optical methods (Xu et al., 2006; Cao et al., 2007; Jimenez et al., 2009). There remains poor agreement between measurements of BC and EC among available measurement techniques. The general techniques used to quantify the various fractions of BC mass concentrations are associated with the corresponding methods: thermal–optical methods, single-particle soot photometer (SP2) measurements, and filter-based optical techniques. Besides the above techniques, the aerosol mass

删除的内容： type

spectrometry, electron microscopy, and Raman spectroscopy are also useful and accurate methods to identify the various fractions of carbonaceous aerosols in the atmosphere (Cross et al., 2010; Ivleva et al., 2007; Spencer et al., 2007; Li et al., 2016; Petzold et al., 2013). Among these methods, the thermal–optical approach is regarded as the most effective and reliable for evaluating EC concentrations (Chylek et al., 1987; Cachier and Pertuisot, 1994; Jenk et al., 2006; Legrand et al., 2007; Hadley et al., 2010). However, the thermal–optical method can lead to large discrepancies in determining EC concentrations as a result of inference from positive artifacts caused by inadequately separated organics and mineral dust (Ballach et al., 2001; Wang et al., 2012). Further discrepancies are caused by the use of two main detection protocols [thermal–optical transmission (TOT) and thermal–optical reflectance (TOR)] to assess EC and OC concentrations based on their unique thermal properties. These protocols yield different OC and EC concentrations (Chow et al., 1993, 2001; Birch and Cary, 1996; Watson and Chow, 2002). The Integrating Sphere/Integrating Sandwich Spectrophotometer (ISSW) method was developed by Grenfell et al. (2011) and has been used to analyze mass concentrations of BC in snow (Doherty et al., 2010, 2014; Wang et al., 2013). Doherty et al. (2010) noted that the total uncertainty in measuring BC in snow using the ISSW method is up to 40% relative to the gravimetric standards of BC (fullerene soot). The total uncertainty associated with the filter-based ISSW technique on BC concentration determination for ambient snow has previously been estimated as 40 %, which is the sum, in quadrature, of 11% for instrumental uncertainty, 15% for undercatch uncertainty (loss of insoluble light-absorbing impurities), 17% for BC mass absorption coefficient (MAC) uncertainty, and 30% for uncertainty in the AAE of non-BC material (Doherty et al., 2010; Grenfell et al., 2011; Schwarz et al., 2012). Finally, the SP2 technique is well suited to the quantification of low BC concentrations with small particle radius (<500 nm). It is an optimized method for measuring BC concentrations and size distributions, and the substantially larger uncertainty of the SP2 instrument with respect to BC concentration measurements can exceed 60% in snow and ice cores, and 30% for atmospheric sampling (Schwarz et al., 2012). They noted that the relative transmission efficiencies of polystyrene latex sphere concentration standards (PSLs) in liquid to the SP2 after

删除的内容: i

aerosolization remarkably reduce to 20% due to larger diameter of BC particles (> 500 nm). Therefore, the larger diameter of BC (>500 nm) is hardly captured by SP2 instrument with a collison-type nebulizer. Moreover, the mixing status of BC in snow is more complicated than the standard fullerene soot in the laboratory and the typical BC in the atmosphere.

带格式的: 字体: (默认) Times New Roman

Although several field campaigns have collected atmospheric, snow, and ice core samples to measure BC and EC concentrations globally (Wolff and Cachier, 1998; von Schneidemesser et al., 2009; Doherty et al., 2010, 2014; Ming et al., 2010; Huang et al., 2011; Xu et al., 2012; Cong et al., 2015), biases remain in determinations of BC concentrations, as is evident from a comparison among the results obtained with the SP2, ISSW, and thermal–optical methods (Schwarz et al., 2012; Lim et al., 2014). As a result, it is difficult to assess the effects of BC and EC on recent climate change using different techniques, even in the same area.

Here we report the development of a new portable and accurate spectrophotometric method based on the two-sphere integration (TSI) technique that can be used to determine BC concentrations in both the atmosphere and seasonal snow. The improved TSI technique minimizes scattering effects related to BC and non-BC insoluble particles collected on Nuclepore filters, and thus provides a simple and accurate means to assess BC concentrations in the atmosphere and seasonal snow. To assess the accuracy of the new technique, a two-step thermal–optical method is applied to determine BC concentrations on individual quartz fiber filters. Finally, we investigate the spatial distribution of BC concentrations and the relative light absorption of surface snow over northeast China. We also analyze the diurnal variations of BC in the atmosphere during day and night over Lanzhou in northwest China.

2 Experimental Procedures

2.1 Sampling sites and snow-sample filtration

During the study period, less snow fell in 2014 than in 2010, and no seasonal snow was present in the western part of Inner Mongolia. Therefore, we collected 94 snow samples

at 14 sites in January and February of 2014 across north China following the sampling route of Huang et al. (2011). The sites are numbered in chronological order from 90 to 103, following previous snow surveys (Ye et al., 2012; Wang et al., 2013). Figure 1 shows the locations of the snow field campaigns across northern China. The sampling locations were selected to be at least 50 km from any settlement and 1 km from the nearest road. Snow samples were kept frozen before being filtered. We set up a temporary laboratory along the sampling route. Owing to BC in snow is often hydrophobic, long time melting could lose more BC to the container walls instead of collected on the filter (Ogren et al., 1983). In order to minimize the loss of insoluble ILAPs, we quickly melted the snow samples in a microwave within a very short time. Therefore, the loss of insoluble LAPs is very limited, and can be neglectable. At present, this method is widely performed for snow melting procedure. (Dothery et al., 2010, 2014; Wang et al.,2013). Subsequently, we simultaneously filtered the snow samples using quartz fiber filters with 1-μm pores and Nuclepore filters with 0.4-μm pores. Then, we refiltered the snow samples for the quartz fiber filters using Nuclepore filters with 0.4-μm pores to account for the loss of BC mass in the 1-μm pore quartz fiber filters. Finally, we stored the original and refiltered snow samples in clean high-density polyethylene bottles in a freezer at −30°C for subsequent analysis. For details of the sampling and filtration procedures, see Wang et al. (2013).

删除的内容: At

删除的内容: set up

删除的内容: ,

删除的内容: the snow samples were quickly melted in a microwave.

带格式的: 字体: Times New Roman, 字体颜色: 文字 1

带格式的: 字体: Times New Roman, 字体颜色: 文字 1

带格式的: 字体: Times New Roman, 字体颜色: 文字 1

带格式的: 字体: Times New Roman, 字体颜色: 文字 1

To evaluate the accuracy of the TSI technique in measuring BC concentrations, the atmospheric samples were collected continuously on Nuclepore and quartz fiber filters with high-volume samplers during the periods 09:00 to 17:00 (daytime; local time) and 23:00 to 07:00 (nighttime) at site 103 in Lanzhou from 5 to 25 August 2015. The pumps were operated at a flow rate of 10 L min^{-1}. In total, 40 atmospheric samples were collected during this experiment and used to assess the accuracy of the atmospheric BC concentration measurements of the improved TSI technique.

2.2 Two-sphere integration technique

Light transmission techniques are the most commonly used methods for determining light-absorbing impurities in aerosol filter samples of the atmosphere and snow/ice. Since the 1970s, a series of optical attenuation techniques have been developed for estimating

BC concentrations using light transmission changes through filters, based on Beer's law. An integrating sphere (IS) technique was first proposed for measuring BC by Fischer (1970). The integrating sphere was coated with diffusely reflecting white paint through a small hole, and the reduction in signal after measuring the sample filters represented the absorption of BC. Subsequently, a new integrating plate (IP) instrument was developed to measure scavenging BC on filters based on the IS technique, which uses a light-diffusing support to provide a nearly Lambertian light source for light transmission using 0.4-μm Nuclepore filters (Clarke et al., 1987; Horvath, 1993b). However, the multiple scattering of solar radiation affect the accuracy of the IP technique (Clarke et al., 1987; Hitzenberger, 1993; Petzold et al., 1997; Bond et al., 1999). A new integrating-sandwich configuration of the ISSW instrument was designed to measure the absorption of light-absorbing impurities based on the ISSW principle of Grenfell et al. (2011). The ISSW instrument can isolate the absorption properties of light-absorbing impurities deposited on polycarbonate Nuclepore filters. By assuming the mass absorption efficiency and non-BC Ångström exponent at 550 nm, this technique is currently capable of reliably measuring BC and non-BC light absorption (Wang et al., 2013; Dang and Hegg, 2014; Doherty et al., 2014). However, Schwarz et al. (2012) found that the total instrumental uncertainty associated with ISSW BC concentration determinations for ambient snow is 11%, and that this uncertainty is partially due to the scattering effects of insoluble impurities deposited on the filters (Doherty et al., 2010; Grenfell et al., 2011).

The improved TSI spectrophotometer developed in this study is small, lightweight, and portable, and can accurately quantify BC concentrations using a technique based on the integrating sphere and integrating plate transmission techniques (Fig. 2). The major improvement of this spectrophotometer is that we replaced the integrating sandwich of the ISSW instrument developed by Grenfell et al. (2011) with a new integrating sphere. In addition, an iron hoop is applied to the top integrating sphere surrounding the sapphire windows to reduce light scattering due to insoluble particles on the filters. Therefore, the total relative light absorption due to all insoluble impurities on the filter can be estimated from the visible-to-near-infrared wavelengths. The total light attenuation can be calculated from the light transmitted by a snow or atmospheric sample, $S(\lambda)$, compared

with that transmitted by a blank filter, $S_0(\lambda)$. Then, the relative attenuation (Atn) through the filter can be expressed as follows

$$Atn = -\ln[S(\lambda)/S_0(\lambda)] \quad (1)$$

Then, the total absorption Ångström exponent $Å_{tot}(\lambda_0)$ of all the ILAPs on the filters can be calculated from the following formula:

$$Å_{tot}(\lambda_0) = -\frac{\ln[\tau_{tot}(\lambda_1)/\tau_{tot}(\lambda_2)]}{\ln(\lambda_1/\lambda_2)} \quad (2)$$

$Å_{non-BC}$ is calculated as a linear combination of the contributions to light absorption made by OC and Fe:

$$Å_{non-BC} = Å_{OC} \times f_{OC} + Å_{Fe} \times f_{Fe} \quad (3)$$

The total absorption Ångström exponent of all ILAPs on a filter ($Å_{tot}$) can be described as a linear combination of $Å_{BC}$ and $Å_{non-BC}$ weighted by the light absorption fraction:

$$Å_{tot}(\lambda_0) = Å_{BC} \times f_{BC}(\lambda_0) + Å_{non-BC} \times f_{non-BC}(\lambda_0) \quad (4)$$

Using the mass absorption efficiency and absorption Ångström exponents for BC, OC, and Fe described by Wang et al. (2013), we can further estimate the following parameters: equivalent BC (C_{BC}^{equiv}), maximum BC (C_{BC}^{max}), estimated BC (C_{BC}^{est}), fraction of light absorption by non-BC ILAPs (insoluble light-absorbing particles) (f_{non-BC}^{est}), absorption Ångström exponent of non-BC ILAPs ($Å_{non\text{-}BC}$), and total absorption Ångström exponent ($Å_{tot}$). These parameters are defined as follows.

1. C_{BC}^{equiv} (ng g^{-1}): *equivalent BC* is the amount of BC that would be needed to produce the total light absorption by all insoluble particles in snow for wavelengths of 300–750 nm.
2. C_{BC}^{max} (ng g^{-1}): *maximum BC* is the maximum possible BC mixing ratio in snow, assuming that all light absorption is due to BC at wavelengths of 650–700 nm.
3. C_{BC}^{est} (ng g^{-1}): *estimated BC* is the estimated true mass of BC in snow derived by separating the spectrally resolved total light absorption and non-BC fractions.
4. f_{non-BC}^{est} (%): the *fraction of light absorption by non-BC light-absorbing particles* is the integrated absorption due to non-BC light-absorbing particles. This value is weighted by the down-welling solar flux at wavelengths of 300–750 nm.

5. $Å_{non\text{-}BC}$: the *non-BC absorption Ångström exponent* is derived from the light absorption by non-BC components for wavelengths of 450–600 nm.

6. $Å_{tot}$: the *absorption Ångström exponent* is calculated for all insoluble particles deposited on the filter between 450 and 600 nm.

Furthermore, combining with the mass loading of Fe was determined by chemical analysis (Wang et al., 2013), the mass loading of OC (L_{OC}) was also estimated assuming that the MAC for OC is 0.3 m^2 g^{-1} at the wavelength of 550 nm using the following equation:

$$\tau_{tot}(\lambda) - MAC_{BC}(\lambda) \times L_{BC}^{est} - MAC_{Fe} \times L_{Fe} = MAC_{OC} \times L_{OC} \qquad (5)$$

All relevant equations and associated derivations are described by Grenfell et al. (2011) and Doherty et al. (2010, 2014). Note that the calculation of non-BC light absorption due to insoluble impurities assumes that the iron in snow is predominantly from mineral dust (Wang et al., 2013).

2.3 Calibration of the TSI spectrophotometer

In this study, a series of 15 Nuclepore filters with a pore size of 0.2 μm (LOT# 7012284, 25mm, Whatman) loaded with fullerene soot (stock #40971, lot #L20W054, Alfa Aesar, Ward Hill, MA, USA) is used to calibrate the spectrophotometer over the range 0.63–38.6 μg, which typically covers >75% of ambient accumulation mode mass (left panel in Table 1; Schwarz et al., 2012). Fullerene soot is commonly used for calibrating the light transmission and thermal–optical techniques for measuring BC concentrations (Baumgardner et al., 2012). Standard fullerene soot particles are fractal-like aggregates of spherical primary particles with a diameter of ~50 nm, with a mean density of 1.05 g cm^{-3} (Moteki et al., 2009). Multiple filters with various loadings are required, as the system response deviates from Beer's law exponential behavior; related equations can be found in Grenfell et al. (2011). Note that uncertainties in mass absorption efficiencies, which range from 2 to 25 m^2 g^{-1}, can lead to uncertainty in this technique. Here, we use a mass absorption efficiency of 6.22 m^2 g^{-1} at 525 nm, which is consistent with Doherty et al. (2010) and Grenfell et al. (2011). Figure 3 shows the best-fit curve (solid line) of loading of the filters at 550 nm. When the filter loading was

删除的内容: mass absorption coefficient (

删除的内容:)

删除的内容: 2

0–40 μg cm^{-2}, all measured results were close to the best-fit curve, indicating that the TSI spectrophotometer is stable and accurate in terms of BC mass measurements.

2.4 Thermal–optical measurements of EC concentration

There are several types of thermal–optical method that can be used to quantify EC and OC concentrations, including two-step temperatures in oxidizing/non-oxidizing atmospheres (Cachier et al., 1989; Xu et al., 2006, 2009b), thermal–optical reflectance (Chow et al., 1993, 2001; Chen et al., 2004), and thermal–optical transmittance (Sharma et al., 2002; Yang and Yu, 2002; Chow et al., 2004). Using an optimized two-step method, Cachier et al. (1989) first confirmed that soot carbon not only comprises EC, but is also mixed with highly condensed organic material. An optimized two-step thermal–optical system has been developed to detect EC and OC concentrations in ice cores (Xu et al., 2006). Here, we use the optimized two-step method based on the thermal–optical technique to measure EC concentrations. In this experiment, quartz fiber filters were first preheated in a muffle furnace at 350°C to remove organic carbon prior to sampling. All filters were punched to yield appropriately sized samples for analysis. Snow samples were analyzed for EC and OC concentrations using a Thermal–Optical Carbon Analyzer (Desert Research Institute, Model 2001A), following the thermal–optical reflectance (TOR) protocol of the Interagency Monitoring of Protected Visual Environments (IMPROVE_A). We developed a new method, referred to as the two-step method, to measure the concentrations of BC collected by the quartz fiber filters. The two-step method is an updated measurement procedure that first extracts an OC fraction below 550°C in a He atmosphere. The volatilized OC is oxidized to CO_2, reduced to CH_4, and detected by a flame ionization system. Next, two EC fractions (EC1 and EC2) are extracted above 550°C in an atmosphere of 2% O_2 and 98% He. Detailed procedures can be found in Xu et al. (2006) and Chow et al. (2004). The analytical uncertainty of this method is 15% for BC and 16% for OC measured via four parallel ice samples cut lengthways in an ice core with high dust loading (Xu et al., 2009a).

3 Results

3.1 Comparison with theoretical calculations

To further assess the accuracy of the TSI system, we use standard fullerene soot and quantify BC concentrations using theoretical calculations for comparison with BC values measured by a laboratory-based TSI spectrophotometer. To ensure the stability and accuracy of the improved TSI spectrophotometer, two individual sets of standard BC filters were used: 0.4-μm Nuclepore and 1-μm quartz fiber filters. All filters were preheated in a muffle furnace at 350°C to remove organic carbon prior to sampling. A measured amount of BC was mixed into a known volume of ultrapure water. The mixture was then agitated by ultrasound for ~10 min, and the same volumes of liquid were then filtered through the two types of filter. Using the calculated BC mass, seven filters with gradually increasing BC concentrations were obtained for both the 0.4-μm Nuclepore and 1-μm quartz fiber filters. Next, all the filters were placed in a dryer for 24 h and then measured using the TSI spectrophotometer. Using the BC mass and the volume of the ultrapure water used for filtration, we can estimate the theoretical BC concentration for each filter. The mass for each filter is listed in Table 1 (right panel).

Assuming a mass absorption cross-section (MAC) of BC of 6.22 m^2 g^{-1} at 525 nm, the BC concentrations measured using the TSI spectrophotometer were in good agreement with the theoretical BC values in the slope of 1.07 (Figure 4). The BC mass loaded on the Nuclepore filters was approximately equal to that measured by the improved TSI spectrometer, which indicates that the TSI system developed here can accurately measure BC concentrations with the assumed mass absorption efficiency. In contrast, the standard BC mass on the quartz fiber filters was underestimated by 35%–45% using the two-step thermal–optical technique, compared with the theoretical value. During the filtration process, we found that the time required to filter liquid snow samples on the 0.4-μm Nuclepore filters was much longer than was the case for the 1-μm quartz fiber filters. Therefore, we first filtered the melted snow samples on the quartz fiber filters, and then re-filtered the snow samples using the 0.4-μm Nuclepore filters. Using this process, BC mass losses can be obtained using the TSI technique, assuming optical BC is equivalent to thermal EC.

删除的内容: (

删除的内容:)

删除的内容: shown in

As shown in Figure 5, the fraction of BC mass collected during the second filtration (0.4-μm filter) ranges from 12% to 21% of the total collected mass (filter directly with 0.4-μm filters), as might be expected for the small particles of standard fullerene soot (<50 nm). This under-sampled fraction decreases with increasing BC mass on the filters, possibly owing to blocking of the filter pores. As a result, the under-sampled fraction of the thermal–optical method was larger than that of the TSI technique, leading to a lower filtration efficiency. Note that these sampling efficiencies are strongly related to the BC size distribution. Therefore, the improved TSI technique developed here is more stable and accurate for measuring pure BC masses, and the data obtained using this method can be used as the standard BC mass. After correcting for systematic biases, the results of both methods were closer to the theoretical BC calculations. Note, however, that the size distribution of the laboratory BC standard was much smaller than those of the atmospheric and seasonal snow samples (Schwarz et al., 2012). Therefore, underestimates caused by the filtration efficiency for ambient BC should be lower than that for the standard BC.

3.2 Comparison of BC concentrations in seasonal snow and the atmosphere

Recent studies have indicated that mineral dust can affect the accurate detection of BC concentrations using the ISSW and thermal–optical methods (Wang et al., 2012; Zhou et al., 2017). To eliminate the large uncertainty and bias due to dust particles, we only used snow samples collected in industrial areas over northeastern China, where the light absorption was dominated by fine-mode ILAPs (e.g., BC and OC; Wang et al., 2013). Hence, most of the snow samples did not contain very large coarse-mode particles, such as mineral and local soil dust.

During the snow field campaign, two series of snow samples were filtered through the Nuclepore and quartz fiber filters and measured using the TSI and two-step thermal–optical methods (Fig. 6). Result shows that most of the BC values measured by the TSI and two-step thermal–optical methods are close to the 1:1 line in a comparison plot, and are generally in good agreement (slope of 1.11, $R^2 = 0.93$, n = 22). However, some BC values in seasonal snow measured by the two-step thermal–optical method are much larger than those measured by the TSI technique. Consequently, for each sample the

mean ratio of BC concentrations measured by the two-step method and the TSI spectrophotometer varies from 0.64 to 3.97, with an overall mean of 1.57. This discrepancy arises from two factors. First, Wang et al. (2017) found that snow grain sizes varied considerably (from 0.07 to 1.3 mm) during this snow field campaign. This range is much larger than that recorded in previous studies, owing to snow melting by solar radiation and ILAPs (Hadley and Kirchstetter, 2012; Painter et al., 2013; Yasunari et al., 2013; Pedersen et al., 2015). These results agree well with those of Schwarz et al. (2012), who found that the sizes of BC particles in snow are much larger than those in typical ambient air. Therefore, the sampling efficiency of the quartz fiber filters could have been significantly higher than expected. The other factor is that the insoluble light-absorbing impurities in seasonal snow over northeast China contained not only BC, but also insoluble organic carbon. This result is consistent with a previous study by Chow et al. (2004), who reported that the charring observed when employing the two-step thermal–optical method at higher temperatures (>550°C) was incomplete and that certain organic compounds are not completely pyrolyzed below 550°C. Therefore, incomplete charring of absorbed organic compounds by the two-step processes may lead to incompletely pyrolyzed OC on the filters, artificially contributing to the BC concentration. This may explain why the BC concentration measured using the thermal–optical method was higher than that measured using the TSI spectrophotometer.

A comparison of BC concentrations in the atmosphere measured by the ISSW and thermal–optical methods is vastly different than that for the snow samples (Fig. 7). Results are in excellent agreement for BC concentrations of <3 μg m^{-3}. However, biases increased gradually with increasing BC concentrations, leading to two-step-to-TSI ratios as low as 0.5. The BC concentrations of >3 μg m^{-3} obtained using the two-step thermal–optical method are much lower than those measured using the improved TSI technique, possibly due to the small particle sizes in the atmosphere, which lead to a lower filtration efficiency. Overall, we conclude that the improved TSI method is more stable and suitable for measuring BC concentrations in both the atmosphere and snow samples compared with the two-step thermal–optical method.

3.3 Spatial distribution of BC and non-BC light absorption measured by the TSI spectrophotometer

The above results show that the improved TSI method measures BC concentrations in the atmosphere and snow/ice with higher accuracy than Two-step thermal optical methods. In this section we investigate the spatial distribution of BC concentrations and their relative light absorption due to BC and non-BC snow impurities in seasonal snow over northeast China during January–February 2014. All BC mass concentrations in surface snow measured by the TSI and thermal–optical methods during the snow field campaigns are listed in Table 2. There was less snow fall in January 2014 than in 2010, and seasonal snow did not cover all of central Inner Mongolia during this time. Thus, we only collected snow samples at site 90. Given that this region is windy, the surface snow collected included drifted and aged snow. The surface BC concentration was 350 ng g^{-1} in the central Inner Mongolia region. The lowest BC concentrations in surface snow, 55 and 280 ng g^{-1}, were found on the border of northeast China (sites 91–97). We note that there were considerable variations in BC concentrations in these regions. The median BC concentration was 1100 ng g^{-1} with a range of 520–3900 ng g^{-1} for surface snow in northeast industrial regions. On 10 February 2014, fresh snow samples were collected in Lanzhou, at a mean snow depth of 6–8 cm. The mean BC concentration in these fresh snow samples from Lanzhou was ~170 ng g^{-1}.

The relative light absorption due to BC and non-BC fractions in seasonal snow measured using the improved TSI technique across northern China is shown in Figure 8. A similar pattern for the light absorption of BC (~70%) and non-BC (~30%) from insoluble light-absorbing impurities in surface snow indicates a similar pollution emission source over northeast China. However, the light absorption due to BC in seasonal snow plays a dominant role (43.11%–88.56%, with a mean of 73.10%). The largest BC light absorption was at site 102. This site is located in the central part of Jilin province, which is polluted by heavy industrial activity. For one sample, the light absorption of non-BC impurities in seasonal snow reached 56.89%, which is the only time it exceeded BC light-absorption. Biomass burning and fossil fuel are likely the major emission sources during the winter in Lanzhou, unlike the case over northeast

删除的内容: 80
删除的内容: 20
删除的内容: 52.3
删除的内容: 93.3
删除的内容: 75.8
删除的内容: 52.3

China. These results are consistent with those of Wang et al. (2013), who found that snow particle light absorption was dominated by BC in northeast China in 2010.

Finally, we investigate atmospheric BC mass concentrations and their relative light absorption measured by the TSI spectrophotometer in Lanzhou during 5–25 August 2015. During this experiment, there were no noticeable trends of BC concentrations in Lanzhou. However, a notable feature in Figure 9 is that the BC mass concentrations at night are generally much higher than during the day (Table 3). The unique topography of Lanzhou likely plays an important role in this phenomenon. Lanzhou is situated in a valley basin with low rainfall, high evaporation, low wind speeds, and high calm-wind frequency, which often leads to a thick inversion layer in which air pollutants accumulate during the night. The light absorption due to BC in the atmosphere ranges from 62.76% to 91.84%, with a mean of 75.43%.

删除的内容: 68.5

删除的内容: 93.29

删除的内容: 77.9

4 Conclusions

We developed an improved two-sphere integration (TSI) spectrophotometer to quantify BC concentrations in snow and atmospheric samples over northern China. The TSI technique significantly reduces scattering effects caused by insoluble impurities deposited on filters. Therefore, the system more accurately measures light absorption due to BC and non-BC impurities. A system calibration using theoretical calculations for standard fullerene soot revealed that the TSI system can be used to assess BC concentrations with low uncertainty. A laboratory comparison revealed that the thermal–optical method can lead to a significant underestimate (35%–45%) of BC concentrations for small-diameter particles (~50 nm) due to the low filtration efficiency of 1-μm quartz fiber filters.

To further assess the accuracy of the improved TSI system, two field campaigns were carried out to collect seasonal snow and atmospheric samples during January–February 2014 and 5–25 August 2015 across northern China, respectively. Although the BC concentrations measured by the TSI and thermal–optical methods are well correlated for both the snow and atmospheric samples, we find that some BC values in seasonal snow measured by the two-step thermal–optical method were significantly overestimated compared with those measured by the TSI technique, by a factor of 1.57. Overall, the

improved TSI optical system developed here is applicable to quantifications of BC concentrations in the atmosphere and snow/ice.

The spatial distribution of BC concentrations in seasonal snow over northern China during January–February 2014 ranged from 60 to 3800 ng g^{-1}, with a mean value of 700 ng g^{-1}, and ranged from 0.78 to 7.75 μg m^{-3} in the atmosphere during 5–25 August 2015 in Lanzhou. The spatial distribution of BC concentrations shows that large BC values are found mainly in the center of industrial regions near the central part, whereas lower values are found in northeast China. Light absorption is dominated by BC (~40% to 90%) in seasonal snow over northeast China, and this plays a dominant role in accelerating snow melt. Atmospheric samples collected in Lanzhou show significant changes in BC concentrations between day and night. Frequent, stable atmospheric boundary layers at night during summer, caused by the valley-basin topography of Lanzhou, are largely responsible for air pollutant accumulation during the night.

删除的内容: 50

删除的内容: 95

Data availability. Data used in this paper are available upon request from corresponding author (wxin@lzu.edu.cn).

Author contributions. The conceptualization and methodology were done by XW. The experiments were designed by XZ and WD. The formal analysis, investigation, writing of the original draft, and editing were performed by XW.

Competing interests. The authors declare that they have no conflict of interest.

Acknowledgements. We thank Thomas C. Grenfell and Qiang Fu from University of Washington for providing the standard filters.

Financial support. This research was supported jointly by the National Key R&D Program of China (2019YFA0606801), the National Natural Science Foundation of

带格式的: 不对齐到网格

China (41975157, 41775144, 41675065, and 41875091), and the Fundamental Research Funds for the Central Universities (lzujbky-2018-k02).

删除的内容: *Financial support.* This research was supported by the National Key Research and Development Program on Monitoring, Early Warning and Prevention of Major Natural Disaster (2018YFC1506005), the National Natural Science Foundation of China (41775144, 41675065, and 41875091), and the Fundamental Research Funds for the Central Universities (lzujbky-2018-k02).

References

Andreae, M.O. and Gelencser, A.: Black carbon or brown carbon? The nature of light-absorbing carbonaceous aerosols, Atmos. Chem. Phys., 6, 3131-3148, doi: 10.5194/acp-6-3131-2006, 2006.

Ban-Weiss, G.A., Cao, L., Bala, G., and Caldeira, K.: Dependence of climate forcing and response on the altitude of black carbon aerosols, Clim. Dyn., 38, 897-911, doi: 10.1007/s00382-011-1052-y, 2012.

Ballach, J., Hitzenberger, R., Schultz, E., and Jaeschke, W.: Development of an improved optical transmission technique for black carbon (BC) analysis, Atmos. Environ. , 35, 2089-2100, doi: 10.1016/S1352-2310(00)00499-4, 2001.

Baumgardner, D., Kok, G., and Raga, G.: Warming of the Arctic lower stratosphere by light absorbing particles, Geophys. Res. Lett., 31, doi: 10.1029/2003GL018883, 2004.

Baumgardner, D., Popovicheva, O., Allan, J., Bernardoni, V., Cao, J., Cavalli, F., Cozic, J., Diapouli, E., Eleftheriadis, K., Genberg, P.J., Gonzalez, C., Gysel, M., John, A., Kirchstetter, T.W., Kuhlbusch, T.A.J., Laborde, M., Lack, D., Muller, T., Niessner, R., Petzold, A., Piazzalunga, A., Putaud, J.P., Schwarz, J., Sheridan, P., Subramanian, R., Swietlicki, E., Valli, G., Vecchi, R., and Viana, M.: Soot reference materials for instrument calibration and intercomparisons: a workshop summary with recommendations, Atmos. Meas. Tech., 5, 1869-1887, doi: 10.5194/amt-5-1869-2012, 2012.

Birch, M.E.: Analysis of carbonaceous aerosols: interlaboratory comparison, Analyst 123, 851-857, doi: 10.1039/A800028J, 1998.

524 Birch, M. E., and Cary, R. A.: Elemental carbon-based method for monitoring
525 occupational exposures to particulate diesel exhaust, Aerosol Sci. Technol., 25,
526 221-241, doi: 10.1080/02786829608965393, 1996.
527 Bond, T.C., Bussemer, M., Wehner, B., Keller, S., Charlson, R.J., and Heintzenberg, J.:
528 Light absorption by primary particle emissions from a lignite burning plant,
529 Environ. Sci. Technol., 33, 3887-3891, doi: 10.1021/es9810538, 1999.
530 Bond, T.C., Streets, D.G., Yarber, K.F., Nelson, S.M., Woo, J.H., and Klimont, Z.: A
531 technology-based global inventory of black and organic carbon emissions from
532 combustion, J. Geophys. Res.-Atmos., 109, doi:10.1029/2003JD003697, 2004.
533 Bond, T.C., Doherty, S.J., Fahey, D.W., Forster, P.M., Berntsen, T., DeAngelo, B.J.,
534 Flanner, M.G., Ghan, S., Karcher, B., Koch, D., Kinne, S., Kondo, Y., Quinn, P.K.,
535 Sarofim, M.C., Schultz, M.G., Schulz, M., Venkataraman, C., Zhang, H., Zhang, S.,
536 Bellouin, N., Guttikunda, S.K., Hopke, P.K., Jacobson, M.Z., Kaiser, J.W., Klimont, Z.,
537 Lohmann, U., Schwarz, J.P., Shindell, D., Storelvmo, T., Warren, S.G., and Zender,
538 C.S.: Bounding the role of black carbon in the climate system: A scientific
539 assessment, J. Geophys. Res.-Atmos., 118, 5380-5552, doi: 10.1002/jgrd.50171,
540 2013.
541 Cachier, H., Bremond, M.P., and Buat-Menard, P.: Determination of atmospheric soot
542 carbon with a simple thermal method, Tellus B., 41, 379-390, doi:
543 10.1111/j.1600-0889.1989.tb00316.x , 1989.
544 Cachier, H. and Pertuisot, M.H.: Particulate Carbon in Arctic Ice, Analusis, 22,
545 M34-M37, 1994.
546 Cao, J.J., Lee, S.C., Ho, K.F., Zhang, X.Y., Zou, S.C., Fung, K., Chow, J.C., and Watson, J.G.:
547 Characteristics of carbonaceous aerosol in Pearl River Delta Region, China during
548 2001 winter period, Atmos. Environ., 37, 1451-1460, doi:
549 10.1016/S1352-2310(02)01002-6, 2003.
550 Cao, J.J., Wu, F., Chow, J.C., Lee, S.C., Li, Y., Chen, S.W., An, Z.S., Fung, K.K., Watson, J.G.,
551 Zhu, C.S., and Liu, S.X.: Characterization and source apportionment of atmospheric
552 organic and elemental carbon during fall and winter of 2003 in Xi'an, China,
553 Atmos. Chem. Phys., 5, 3127-3137, doi: 10.5194/acp-5-3127-2005, 2005.

554 Cao, J.J., Lee, S.C., Chow, J.C., Watson, J.G., Ho, K.F., Zhang, R.J., Jin, Z.D., Shen, Z.X., Chen,
555 G.C., Kang, Y.M., Zou, S.C., Zhang, L.Z., Qi, S.H., Dai, M.H., Cheng, Y., and Hu, K.:
556 Spatial and seasonal distributions of carbonaceous aerosols over China, J.
557 Geophys. Res.-Atmos., 112, doi: 10.1029/2006JD008205, 2007.
558 Carmagnola, C.M., Domine, F., Dumont, M., Wright, P., Strellis, B., Bergin, M., Dibb, J.,
559 Picard, G., Libois, Q., Arnaud, L., and Morin, S.: Snow spectral albedo at Summit,
560 Greenland: measurements and numerical simulations based on physical and
561 chemical properties of the snowpack, The Cryosphere, 7, 1139-1160, doi:
562 10.5194/tc-7-1139-2013, 2013.
563 Chen, L.W.A., Chow, J.C., Watson, J.G., Moosmuller, H., and Arnott, W.P.: Modeling
564 reflectance and transmittance of quartz-fiber filter samples containing elemental
565 carbon particles: Implications for thermal/optical analysis, J. Aerosol Sci., 35,
566 765-780, doi: 10.1016/j.jaerosci.2003.12.005, 2004.
567 Chow, J.C., Watson, J.G., Pritchett, L.C., Pierson, W.R., Frazier, C.A., and Purcell, R.G.:
568 The Dri Thermal Optical Reflectance Carbon Analysis System - Description,
569 Evaluation and Applications in United-States Air-Quality Studies, Atmos. Environ.,
570 27, 1185-1201, doi: 10.1016/0960-1686(93)90245-T , 1993.
571 Chow, J.C., Watson, J.G., Lu, Z.Q., Lowenthal, D.H., Frazier, C. A., Solomon, P. A.,
572 Thuillier, R. H., Magliano, K.: Descriptive analysis of PM(2.5) and PM(10) at
573 regionally representative locations during SJVAQS/AUSPEX. Atmos. Environ., 30,
574 2079-2112, doi: 10.1016/1352-2310(95)00402-5, 1996.
575 Chow, J.C., Watson, J.G., Crow, D., Lowenthal, D.H., and Merrifield, T.: Comparison of
576 IMPROVE and NIOSH carbon measurements, Aerosol Sci. Technol., 34, 23-34, doi:
577 10.1080/02786820119073, 2001.
578 Chow, J.C., Watson, J.G., Chen, L.W.A., Arnott, W.P., Moosmuller, H., and Fung, K.:
579 Equivalence of elemental carbon by thermal/optical reflectance and
580 transmittance with different temperature protocols, Environ. Sci. Technol., 38,
581 4414-4422, doi: 10.1021/es034936u, 2004.
582 Chuang, C.C., Penner, J.E., Prospero, J.M., Grant, K.E., Rau, G.H., and Kawamoto, K.:
583 Cloud susceptibility and the first aerosol indirect forcing: Sensitivity to black

584 carbon and aerosol concentrations, J. Geophys. Res.-Atmos., 107, doi:
585 10.1029/2000JD000215, 2002.
586 Chylek, P., Srivastava, V., Cahenzli, L., Pinnick, R.G., Dod, R.L., Novakov, T., Cook, T.L.,
587 and Hinds, B.D.: Aerosol and Graphitic Carbon Content of Snow, J. Geophys.
588 Res.-Atmos., 92, 9801-9809, doi: 10.1029/JD092iD08p09801, 1987.
589 Clarke, A.D., Noone, K.J., Heintzenberg, J., Warren, S.G., and Covert, D.S.: Aerosol
590 Light-Absorption Measurement Techniques - Analysis and Intercomparisons,
591 Atmos. Environ., 21, 1455-1465, doi: 10.1016/0004-6981(67)90093-5, 1967.
592 Cong, Z., Kang, S., Kawamura, K., Liu, B., Wan, X., Wang, Z., Gao, S., and Fu, P.:
593 Carbonaceous aerosols on the south edge of the Tibetan Plateau: concentrations,
594 seasonality and sources, Atmos. Chem. Phys., 15, 1573-1584, doi:
595 10.5194/acp-15-1573-2015, 2015.
596 Cross, E.S., Onasch, T.B., Ahern, A., Wrobel, W., Slowik, J.G., Olfert, J., Lack, D.A.,
597 Massoli, P., Cappa, C.D., Schwarz, J.P., Spackman, J.R., Fahey, D.W., Sedlacek, A.,
598 Trimborn, A., Jayne, J.T., Freedman, A.,Williams, L.R., Ng, N.L., Mazzoleni, C., Dubey,
599 M., Brem, B., Kok, G., Subramanian, R., Freitag, S., Clarke, A., Thornhill, D., Marr,
600 L.C., Kolb, C.E., Worsnop, D.R., and Davidovits, P.: Soot Particle Studies-Instrument
601 Inter-Comparison-Project Overview, Aerosol Sci. Technol., 44, 592–611, 2010.
602 Dang, C. and Hegg, D.A.: Quantifying light absorption by organic carbon in Western
603 North American snow by serial chemical extractions, J. Geophys. Res.-Atmos., 119,
604 10247-10261, doi: 10.1002/2014JD022156, 2014.
605 Doherty, S.J., Warren, S.G., Grenfell, T.C., Clarke, A.D., and Brandt, R.E.:
606 Light-absorbing impurities in Arctic snow, Atmos. Chem. Phys., 10, 11647-11680,
607 doi: 10.5194/acp-10-11647-2010, 2010.
608 Doherty, S.J., Dang, C., Hegg, D.A., Zhang, R.D., and Warren, S.G.: Black carbon and
609 other light-absorbing particles in snow of central North America, J. Geophys.
610 Res.-Atmos., 119, 12807-12831, doi: 10.1002/2014JD022350, 2014.
611 Fischer K.: Bestimmung der Absorption von sichtbarer Strahlung durch
612 Aerosolpartikeln, Contr. Atmos. Phys., 43, 244-254, 1970.

Flanner, M.G., Liu, X., Zhou, C., Penner, J.E., and Jiao, C.: Enhanced solar energy absorption by internally-mixed black carbon in snow grains, Atmos. Chem. Phys., 12, 4699-4721, doi: 10.5194/acp-12-4699-2012, 2012.

Forsstrom, S., Isaksson, E., Skeie, R.B., Strom, J., Pedersen, C.A., Hudson, S.R., Berntsen, T.K., Lihavainen, H., Godtliebsen, and F., Gerland, S.: Elemental carbon measurements in European Arctic snow packs, J. Geophys. Res.-Atmos., 118, 13614-13627, doi: 10.1002/2013JD019886, 2013.

Gillies, J. A., Gertler, A.W., Sagebiel, J.C., Dippel, W.A.: On-road particulate matter (PM2.5 and PM10) emissions in the Sepulveda Tunnel, Los Angeles, California. Environ. Sci. Technol., 35, 1054-1063, 2001.

Gray, H. A., Cass, G. R., Huntzicker, J. J., Heyerdahl, E.K., Rau, J.A.: Characteristics of Atmospheric Organic and Elemental Carbon Particle Concentrations in Los-Angeles. Environ. Sci. Technol., 20, 580-589, doi: 10.1021/Es00148a006, 1986.

Grenfell, T.C., Doherty, S.J., Clarke, A.D., and Warren, S.G.: Light absorption from particulate impurities in snow and ice determined by spectrophotometric analysis of filters, Appl. Opt., 50, 2037-2048, doi: 10.1364/AO.50.002037, 2011.

Hadley, O.L., Corrigan, C.E., Kirchstetter, T.W., Cliff, S.S., and Ramanathan, V.: Measured black carbon deposition on the Sierra Nevada snow pack and implication for snow pack retreat, Atmos. Chem. Phys., 10, 7505-7513, doi: 10.5194/acp-10-7505-2010, 2010.

Hadley, O.L. and Kirchstetter, T.W.: Black-carbon reduction of snow albedo, Nat. Clim. Chang., 2, 437-440, doi: 10.1038/NCLIMATE1433, 2012.

Han, Y. M., Han, Z. W., Cao, J. J., Chow, J.C., Watson, J.G., An, Z.S., Liu, S.X., Zhang, R.J.: Distribution and origin of carbonaceous aerosol over a rural high-mountain lake area, Northern China and its transport significance. Atmos. Environ., 42, 2405-2414, doi: 10.1016/j.atmosenv.2007.12.020, 2008.

Hansen, A. D. A., Rosen, H., and Novakov, T.: The aethalometer — An instrument for the real-time measurement of optical absorption by aerosol particles, Sci. Total Environ., 36, 191-196, doi: 10.1016/0048-9697(84)90265-1, 1984.

643 Hansen, J., Sato, M., Ruedy, R., Nazarenko, L., Lacis, A., Schmidt, G.A., Russell, G.,
644 Aleinov, I., Bauer, M., Bauer, S., Bell, N., Cairns, B., Canuto, V., Chandler, M., Cheng,
645 Y., Del Genio, A., Faluvegi, G., Fleming, E., Friend, A., Hall, T., Jackman, C., Kelley, M.,
646 Kiang, N., Koch, D., Lean, J., Lerner, J., Lo, K., Menon, S., Miller, R., Minnis, P.,
647 Novakov, T., Oinas, V., Perlwitz, J., Perlwitz, J., Rind, D., Romanou, A., Shindell, D.,
648 Stone, P., Sun, S., Tausnev, N., Thresher, D., Wielicki, B., Wong, T., Yao, M., and
649 Zhang, S.: Efficacy of climate forcings, J. Geophys. Res.-Atmos., 110, doi:
650 10.1029/2005JD005776, 2005.
651 Heintzenberg, J.: Fine particles in the global troposphere A review, Tellus B., 41,
652 149-160, doi: 10.1111/j.1600-0889.1989.tb00132.x, 1989.
653 Hitzenberger, R.: Absorption-Measurements with an Integrating Plate Photometer
654 Calibration and Error Analysis, Aerosol Sci. Technol., 18, 70-84, doi:
655 10.1080/02786829308959585, 1993.
656 Horvath, H.: Comparison of Measurements of Aerosol Optical-Absorption by Filter
657 Collection and a Transmissometric Method, Atmos. Environ., 27, 319-325, doi:
658 10.1016/0960-1686(93)90105-8, 1993a.
659 Horvath, H.: Atmospheric Light-Absorption - a Review, Atmos. Environ., 27, 293-317,
660 doi: 10.1016/0960-1686(93)90104-7, 1993b.
661 Huang, J.P., Fu, Q.A., Zhang, W., Wang, X., Zhang, R.D., Ye, H., and Warren, S.G.: Dust
662 and Black Carbon in Seasonal Snow across Northern China, Bull. Amer. Meteor.
663 Soc., 92, 175-181, doi: 10.1175/2010BAMS3064.1, 2011.
664 IPCC. 2013. Climate Change 2013: The Physical Science Basis[M]. Stocker, T. F., D .
665 Qin, G. K. Plattner, et al., Cambridge, United Kingdom and New York, NY, USA.
666 Ivleva, N. P., McKeon, U., Niessner, R., and Pöschl, U.: Raman microspectroscopic
667 analysis of size-resolved atmospheric aerosol particle samples collected with an
668 ELPI: Soot, humic-like substances, and inorganic compounds, Aerosol Sci.
669 Technol., 41, 655–671, doi:10.1080/02786820701376391, 2007.
670 Jacobson, M.Z.: Strong radiative heating due to the mixing state of black carbon in
671 atmospheric aerosols, Nature 409, 695-697, doi: 10.1038/35055518, 2001a.

672 Jacobson, M.Z.: Global direct radiative forcing due to multicomponent anthropogenic
673 and natural aerosols, J. Geophys. Res.-Atmos., 106, 1551-1568, doi:
674 10.1029/2000JD900514, 2001b.
675 Jenk, T.M., Szidat, S., Schwikowski, M., Gaggeler, H.W., Brutsch, S., Wacker, L., Synal,
676 H.A., and Saurer, M.: Radiocarbon analysis in an Alpine ice core: record of
677 anthropogenic and biogenic contributions to carbonaceous aerosols in the past
678 (1650-1940), Atmos. Chem. Phys., 6, 5381-5390, doi: 10.5194/acp-6-5381-2006,
679 2006.
680 Jimenez, J. L., Canagaratna, M. R., Donahue, N. M., Prevot, A.S.H., Zhang, Q., Kroll, J.H.,
681 DeCarlo, P.F., Allan, J.D., Coe, H., Ng, N.L., Aiken, A.C., Docherty, K.S., Ulbrich, I.M.,
682 Grieshop, A.P., Robinson, A.L., Duplissy, J., Smith, J.D., Wilson, K.R., Lanz, V.A.,
683 Hueglin, C., Sun, Y.L., Tian, J., Laaksonen, A., Raatikainen, T., Rautiainen, J.,
684 Vaattovaara, P., Ehn, M., Kulmala, M., Tomlinson, J.M., Collins, D.R., Cubison, M.J.,
685 Dunlea, E.J., Huffman, J.A., Onasch, T.B., Alfarra, M.R., Williams, P.I., Bower, K.,
686 Kondo, Y., Schneider, J., Drewnick, F., Borrmann, S., Weimer, S., Demerjian, K.,
687 Salcedo, D., Cottrell, L., Griffin, R., Takami, A., Miyoshi, T., Hatakeyama, S., Shimono,
688 A., Sun, J.Y., Zhang, Y.M., Dzepina, K., Kimmel, J.R., Sueper, D., Jayne, J.T., Herndon,
689 S.C., Trimborn, A.M., Williams, L.R., Wood, E.C., Middlebrook, A.M., Kolb, C.E.,
690 Baltensperger, U., Worsnop, D.R.: Evolution of organic aerosols in the atmosphere,
691 Science, 326, 1525–1529, 2009.
692 Koch, D., Schulz, M., Kinne, S., McNaughton, C., Spackman, J.R., Balkanski, Y., Bauer, S.,
693 Berntsen, T., Bond, T.C., Boucher, O., Chin, M., Clarke, A., De Luca, N., Dentener, F.,
694 Diehl, T., Dubovik, O., Easter, R., Fahey, D.W., Feichter, J., Fillmore, D., Freitag, S.,
695 Ghan, S., Ginoux, P., Gong, S., Horowitz, L., Iversen, T., Kirkevag, A., Klimont, Z.,
696 Kondo, Y., Krol, M., Liu, X., Miller, R., Montanaro, V., Moteki, N., Myhre, G., Penner,
697 J.E., Perlwitz, J., Pitari, G., Reddy, S., Sahu, L., Sakamoto, H., Schuster, G., Schwarz,
698 J.P., Seland, O., Stier, P., Takegawa, N., Takemura, T., Textor, C., van Aardenne, J.A.,
699 and Zhao, Y.: Evaluation of black carbon estimations in global aerosol models,
700 Atmos. Chem. Phys., 9, 9001-9026, doi: 10.5194/acp-9-9001-2009, 2009.

Legrand, M., Preunkert, S., Schock, M., Cerqueira, M., Kasper-Giebl, A., Afonso, J., Pio, C., Gelencser, A., and Dombrowski-Etchevers, I.: Major 20th century changes of carbonaceous aerosol components (EC, WinOC, DOC, HULIS, carboxylic acids, and cellulose) derived from Alpine ice cores, J. Geophys. Res.-Atmos., 112, doi: 10.1029/2006JD008080, 2007.

Li, W., Shao, L., Zhang, D., Ro, C.-U., Hu, M., Bi, X., Geng, H., Matsuki, A., Niu, H., and Chen, J.: A review of single aerosol particle studies in the atmosphere of East Asia: morphology, mixing state, source, and heterogeneous reactions, J. Clean Prod., 112, 1330-1349, https://doi.org/10.1016/j.jclepro.2015.04.050, 2016.

Lim, S., Fain, X., Zanatta, M., Cozic, J., Jaffrezo, J.L., Ginot, P., and Laj, P.: Refractory black carbon mass concentrations in snow and ice: method evaluation and inter-comparison with elemental carbon measurement, Atmos. Meas. Tech., 7, 3307-3324, doi: 10.5194/amt-7-3307-2014, 2014.

McMeeking, G.R., Morgan, W.T., Flynn, M., Highwood, E.J., Turnbull, K., Haywood, J., and Coe, H.: Black carbon aerosol mixing state, organic aerosols and aerosol optical properties over the United Kingdom, Atmos. Chem. Phys., 11, 9037-9052, doi: 10.5194/acp-11-9037-2011, 2011.

Menon, S., Hansen, J., Nazarenko, L., Luo, Y.F.: Climate effects of black carbon aerosols in China and India, Science 297, 2250-2253, doi: 10.1126/science.1075159, 2002.

Ming, J., Cachier, H., Xiao, C., Qin, D., Kang, S., Hou, S., and Xu, J.: Black carbon record based on a shallow Himalayan ice core and its climatic implications, Atmos. Chem. Phys., 8, 1343-1352, doi: 10.5194/acp-8-1343-2008, 2008.

Ming, J., Xiao, C.D., Cachier, H., Qin, D.H., Qin, X., Li, Z.Q., and Pu, J.C.: Black Carbon (BC) in the snow of glaciers in west China and its potential effects on albedos, Atmos. Res., 92, 114-123, doi: 10.1016/j.atmosres.2008.09.007, 2009.

Ming, J., Xiao, C.D., Sun, J.Y., Kang, S.C., and Bonasoni, P.: Carbonaceous particles in the atmosphere and precipitation of the Nam Co region, central Tibet, J. Environ. Sci., 22, 1748-1756, doi: 10.1016/S1001-0742(09)60315-6, 2010.

730 Moosmuller, H., Chakrabarty, R.K., and Arnott, W.P.: Aerosol light absorption and its
731 measurement: A review, J. Quant. Spectrosc. Ra., 110, 844-878, doi:
732 10.1016/j.jqsrt.2009.02.035, 2009.
733 Moteki, N., Kondo, Y., Takegawa, N., and Nakamura, S.-i.: Directional dependence of
734 thermal emission from nonspherical carbon particles, J. Aerosol Sci., 40, 790-801,
735 doi: 10.1016/j.jaerosci.2009.05.003, 2009.
736 Murphy, D. M., Cziczo, D. J., Froyd, K. D., Hudson, P. K., Matthew, B. M., Middlebrook,
737 A. M., Peltier, R. E., Sullivan, A., Thomson, D. S., Weber, R. J.: Single-particle mass
738 spectrometry of tropospheric aerosol particles. J. Geophys. Res., 111, D23S32,
739 doi:10.1029/2006JD007340, , 2006.
740 Ogren, J. A. and Charlson, R. J.: Elemental carbon in the atmosphere– cycle and
741 lifetime, Tellus, 35B, 241–254, 1983.
742 Painter, T.H., Seidel, F.C., Bryant, A.C., Skiles, S.M., and Rittger, K.: Imaging
743 spectroscopy of albedo and radiative forcing by light-absorbing impurities in
744 mountain snow, J. Geophys. Res.-Atmos., 118, 9511-9523, doi:
745 10.1002/jgrd.50520, 2013.
746 Pan, Y.P., Wang, Y.S., Xin, J.Y., Tang, G.Q., Song, T., Wang, Y.H., Li, X.R., and Wu, F.K.:
747 Study on dissolved organic carbon in precipitation in Northern China, Atmos.
748 Environ., 44, 2350-2357, doi: 10.1016/j.atmosenv.2010.03.033, 2010.
749 Pavese, G., Calvello, M., and Esposito, F.: Black Carbon and Organic Components in
750 the Atmosphere of Southern Italy: Comparing Emissions from Different Sources
751 and Production Processes of Carbonaceous Particles, Aerosol Air Qual. Res., 12,
752 1146-1156, doi: 10.4209/aaqr.2011.12.0236, 2012.
753 Pedersen, C.A., Gallet, J.C., Strom, J., Gerland, S., Hudson, S.R., Forsstrom, S., Isaksson,
754 E., and Berntsen, T. K.: In situ observations of black carbon in snow and the
755 corresponding spectral surface albedo reduction, J. Geophys. Res.-Atmos., 120,
756 1476-1489, doi: 10.1002/2014jd022407, 2015.
757 Petzold, A., Kopp, C., and Niessner, R.: The dependence of the specific attenuation
758 cross-section on black carbon mass fraction and particle size, Atmos. Environ., 31,
759 661-672, doi: 10.1016/S1352-2310(96)00245-2, 1997.

760 Petzold, A., Ogren, J. A., Fiebig, M., Laj, P., Li, S.-M., Baltensperger, U., Holzer-Popp, T.,
761 Kinne, S., Pappalardo, G., Sugimoto, N., Wehrli, C., Wiedensohler, A., and Zhang,
762 X.-Y.: Recommendations for reporting "black carbon" measurements, Atmos.
763 Chem. Phys., 13, 8365-8379, https://doi.org/10.5194/acp-13-8365-2013, 2013.
764 Qian, Y., Wang, H., Zhang, R., Flanner, M.G., and Rasch, P.J.: A sensitivity study on
765 modeling black carbon in snow and its radiative forcing over the Arctic and
766 Northern China, Environ. Res. Lett., 9, 064001, doi:
767 10.1088/1748-9326/9/6/064001, 2014.
768 Quinn, P. K. and Bates, T. S.: North American, Asian, and Indian haze: Similar
769 regional impacts on climate? Geophys. Res. Lett., 30, 1555,
770 doi:10.1029/2003GL016934, 2003.
771 Ramanathan, V., and Carmichael, G.: Global and regional climate changes due to
772 black carbon, Nat. Geosci. , 1, 221-227, Doi 10.1038/Ngeo156, 2008.
773 Rosenfeld, D., Lohmann, U., Raga, G.B., O'Dowd, C.D., Kulmala, M., Fuzzi, S., Reissell, A.,
774 and Andreae, M.O.: Flood or drought: How do aerosols affect precipitation?
775 Science 321, 1309-1313, doi: 10.1126/science.1160606, 2008.
776 Schmid, H., Laskus, L., Abraham, H.J., Baltensperger, U., Lavanchy, V., Bizjak, M.,
777 Burba, P., Cachier, H., Crow, D., Chow, J., Gnauk, T., Even, A., ten Brink, H.M., Giesen,
778 K.P., Hitzenberger, R., Hueglin, C., Maenhaut, W., Pio, C., Carvalho, A., Putaud, J.P.,
779 Toom-Sauntry, D., and Puxbaum, H.: Results of the "carbon conference"
780 international aerosol carbon round robin test stage I, Atmos. Environ., 35,
781 2111-2121, doi: 10.1016/S1352-2310(00)00493-3, 2001.
782 Schwarz, J.P., Doherty, S.J., Li, F., Ruggiero, S.T., Tanner, C.E., Perring, A.E., Gao, R.S.,
783 and Fahey, D.W.: Assessing Single Particle Soot Photometer and Integrating
784 Sphere/Integrating Sandwich Spectrophotometer measurement techniques for
785 quantifying black carbon concentration in snow, Atmos. Meas. Tech., 5,
786 2581-2592, doi: 10.5194/amt-5-2581-2012, 2012.
787 Sharma, S., Brook, J.R., Cachier, H., Chow, J., Gaudenzi, A., and Lu, G.: Light absorption
788 and thermal measurements of black carbon in different regions of Canada, J.
789 Geophys. Res.-Atmos., 107, doi: 10.1029/2002JD002496, 2002.

790 Slater, J.F., Currie, L.A., Dibb, J.E., and Benner, B.A.: Distinguishing the relative
791 contribution of fossil fuel and biomass combustion aerosols deposited at Summit,
792 Greenland through isotopic and molecular characterization of insoluble carbon,
793 Atmos. Environ., 36, 4463-4477, doi: 10.1016/S1352-2310(02)00402-8, 2002.
794 Spencer, M.T., Shields, L.G., and Prather, K. A.: Simultaneous measurement of the
795 effective density and chemical composition of ambient aerosol particles, Environ.
796 Sci. Technol., 41, 1303–1309, doi:10.1021/es061425+, 2007.
797 Thevenon, F., Anselmetti, F.S., Bernasconi, S.M., and Schwikowski, M.: Mineral dust
798 and elemental black carbon records from an Alpine ice core (Colle Gnifetti glacier)
799 over the last millennium, J. Geophys. Res.-Atmos., 114, doi:
800 10.1029/2008JD011490, 2009.
801 Turpin, B. J., Cary, R. A., and Huntzicker, J. J.: An insitu,time-resolved analyzer for
802 aerosol organic and elemental carbon. Aerosol Sci. Technol., 12, 161-171, doi:
803 10.1080/02786829008959336, 1990.
804 Turpin, B. J., and Huntzicker, J. J.: Secondary formation of organic aerosol in the Los
805 Angeles Basin: A descriptive analysis of organic and elemental carbon
806 concentrations. Atmos. Environ., 25A, 207-215, 1991.
807 von Schneidemesser, E., Schauer, J.J., Hagler, G.S.W., and Bergin, M.H.:
808 Concentrations and sources of carbonaceous aerosol in the atmosphere of Summit,
809 Greenland, Atmos. Environ., 43, 4155-4162, doi: 10.1016/j.atmosenv.2009.05.043,
810 2009.
811 Wang, M., Xu, B., Zhao, H., Cao, J., Joswiak, D., Wu, G., and Lin, S.: The Influence of
812 Dust on Quantitative Measurements of Black Carbon in Ice and Snow when Using
813 a Thermal Optical Method, Aerosol Sci. Technol., 46, 60-69, doi:
814 10.1080/02786826.2011.605815, 2012.
815 Wang, X., Doherty, S.J., and Huang, J.P.: Black carbon and other light-absorbing
816 impurities in snow across Northern China, J. Geophys. Res.-Atmos., 118,
817 1471-1492, doi: 10.1029/2012JD018291, 2013.
818 Wang, X., Pu, W., Ren, Y., Zhang, X.L., Zhang, X.Y., Shi, J.S., Jin, H.C., Dai, M.K., Chen, Q.L.:
819 Observations and model simulations of snow albedo reduction in seasonal snow

820 due to insoluble light-absorbing particles during 2014 Chinese survey, Atmos.
821 Chem. Phys., 17, 2279-2296, doi: 10.5194/acp-17-2279-2017, 2017.
822 Wang, R, Tao, S., Balkanski, Y., Ciais, P., Boucher, O., Liu, J.F., Piao, S.L., Shen, H.Z.,
823 Vuolo, M.R., Valari, M., Chen, H., Chen, Y.C., Cozic, A., Huang, Y., Li, B.A., Li, W., Shen,
824 G.F., Wang, B., Zhang, Y.Y.: Exposure to ambient black carbon derived from a
825 unique inventory and high-resolution model. Proc. Natl. Acad. Sci. USA., 111,
826 2459-2461, doi: 10.1073/pnas.1318763111, 2014.
827 Watson, J. G., and Chow, J. C.: Comparison and evaluation of in situ and filter carbon
828 measurements at the Fresno Supersite, J. Geophys. Res.-Atmos., 107,
829 doi:10.1029/2001jd000573, 2002.
830 Wolff, E.W. and Cachier, H.: Concentrations and seasonal cycle of black carbon in
831 aerosol at a coastal Antarctic station, J. Geophys. Res.-Atmos., 103, 11033-11041,
832 doi: 10.1029/97JD01363, 1998.
833 Xu, B.Q., Yao, T.D., Liu, X.Q., and Wang, N.L.: Elemental and organic carbon
834 measurements with a two-step heating-gas chromatography system in snow
835 samples from the Tibetan Plateau, Annals of Glaciology, Vol 43, 2006 43, 257-262,
836 doi: 10.3189/172756406781812122, 2006.
837 Xu, B.Q., Cao, J.J., Hansen, J., Yao, T.D., Joswia, D.R., Wang, N.L., Wu, G.J., Wang, M.,
838 Zhao, H.B., Yang, W., Liu, X.Q., and He, J.Q.: Black soot and the survival of Tibetan
839 glaciers, Proc. Nat. Acad. Sci. U.S.A., 106, 22114-22118, doi:
840 10.1073/pnas.0910444106, 2009a.
841 Xu, B.Q., Wang, M., Joswiak, D.R., Cao, J.J., Yao, T.D., Wu, G.J., Yang, W., and Zhao, H.B.:
842 Deposition of anthropogenic aerosols in a southeastern Tibetan glacier, J. Geophys.
843 Res.-Atmos., 114, doi: 10.1029/2008JD011510, 2009b.
844 Xu, B.Q., Cao, J.J., Joswiak, D.R., Liu, X.Q., Zhao, H.B., and He, J.Q.: Post-depositional
845 enrichment of black soot in snow-pack and accelerated melting of Tibetan glaciers,
846 Environ. Res. Lett., 7, doi: 10.1088/1748-9326/7/1/014022, 2012.
847 Yang, H., and Yu, J.Z.: Uncertainties in charring correction in the analysis of
848 elemental and organic carbon in atmospheric particles by thermal/optical
849 methods, Environ. Sci. Technol., 36, 5199-5204, doi: 10.1021/es025672z , 2002.

Yasunari, T. J., Tan, Q., Lau, K. M., Bonasoni, P., Marinoni, A., Laj, P., Menegoz, M., Takemura, T., and Chin, M.: Estimated range of black carbon dry deposition and the related snow albedo reduction over Himalayan glaciers during dry pre-monsoon periods, Atmos. Environ., 78, 259-267, doi:10.1016/j.atmosenv.2012.03.031, 2013.

Yasunari, T. J., Koster, R. D., Lau, W. K. M., Kim, K.: Impact of snow darkening via dust, black carbon, and organic carbon on boreal spring climate in the Earth system. J. Geophys. Res.-Atmos., 120, 5485-5503, doi: 10.1002/2014jd022977, 2015.

Ye, H., Zhang, R.D., Shi, J.S., Huang, J.P., Warren, S.G., and Fu, Q.: Black carbon in seasonal snow across northern Xinjiang in northwestern China, Environ. Res. Lett., 7, doi: 10.1088/1748-9326/7/4/044002, 2012.

Zhang, R.J., Ho, K.F., Cao, J.J., Han, Z.W., Zhang, M.G., Cheng, Y., and Lee, S.C.: Organic carbon and elemental carbon associated with PM10 in Beijing during spring time, J. Hazard. Mater., 172, 970-977, doi: 10.1016/j.jhazmat.2009.07.087, 2009.

Zhao, C., Hu, Z., Qian, Y., Leung, L.R., Huang, J., Huang, M., Jin, J., Flanner, M.G., Zhang, R., Wang, H., Yan, H., Lu, Z., and Streets, D.G.: Simulating black carbon and dust and their radiative forcing in seasonal snow: a case study over North China with field campaign measurements, Atmos. Chem. Phys., 14, 11475-11491, doi: 10.5194/acp-14-11475-2014, 2014

Zhou, Y., Wang, X., Wu, X.Q., Cong, Z.Y., Wu, G.M., Ji, M.X.: Quantifying Light Absorption of Iron Oxides and Carbonaceous Aerosol in Seasonal Snow across Northern China, Atmosphere-Basel, 8, doi: 10.3390/atmos8040063, 2017.

Figure captions:

Figure 1 Sampling locations. Sites 90–102 are located in northeast China and were used for snow sample collection during Jan–Feb. 2014. Snow sampling site 103 is located in Lanzhou in northwest China, and was used for atmospheric sample collection during 5–25 August 2015. Sites are numbered according to Wang et al. (2013) and Ye et al. (2012).

Figure 2 Schematic diagram of the improved two-sphere integrating spectrophotometer.

Figure 3 Calibration curve for standard fullerene soot at a wavelength of 550 nm. The solid line is a best-fit curve for the filter measurements. S_0 and S are the detected signals for the blank and sample filters, respectively, and $-\ln(S/S_0)$ is the relative attenuation.

删除的内容: 600

Figure 4 Comparison of the theoretical and measured BC mass determined by the TSI and two-step techniques in the laboratory. The solid and dot–dashed lines represent best-fit lines for the TSI and two-step techniques, respectively. The dashed line is a 1:1 line.

Figure 5 Mass loss of standard fullerene soot on 1.0-μm quartz fiber filters determined by refiltration using 0.4-μm Nuclepore filters.

Figure 6 Comparison of BC concentrations in snow samples over northeast China during January–February 2014 determined by the TSI and two-step thermal optical methods. A 1:1 line (dashed) and a linear regression fit passing through the origin (solid curve) are also shown.

Figure 7 As for Fig. 6, but for atmospheric samples collected at Lanzhou in northwest China during 5–25 August 2015.

Figure 8 Spatial distributions of light absorption at 550 nm due to BC and non-BC fractions in surface snow across northern China during January–February 2014.

Figure 9 Variations in 8-hour (a) BC concentration and (b) BC and non-BC light absorption measured by TSI spectrophotometer at 550 nm at Lanzhou during 5–25 August 2015 (day: 9 am to 5 pm; night: 11 pm to 7 am).

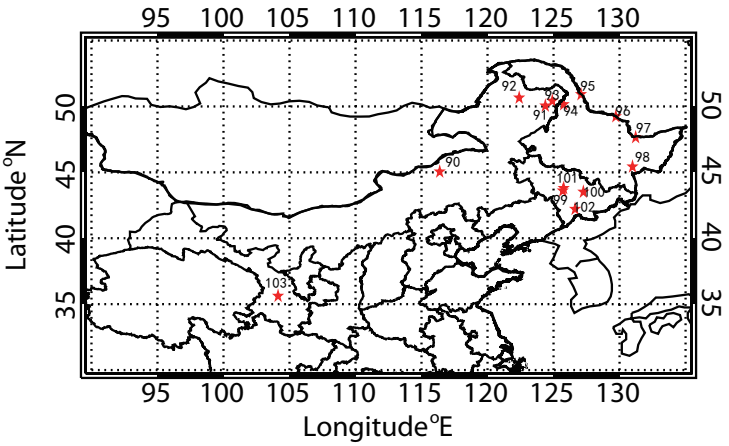

Figure 1 Sampling locations. Sites 90–102 are located in northeast China and were used for snow sample collection during Jan–Feb. 2014. Snow sampling site 103 is located in Lanzhou in northwest China, and was used for atmospheric sample collection during 5–25 August 2015. Sites are numbered according to Wang et al. (2013) and Ye et al. (2012).

Table 1 Series of 15 standard filters loaded with fullerene soot, and a comparison of BC concentrations between theoretical calculations and the TSI/two-step thermal–optical methods in the laboratory.

Filter	Standard BC Concentration ($\mu g/cm^2$)	Filter	Standard BC Concentration ($\mu g/cm^2$)	Filter	Calculated BC (μg)	TSI BC (μg)	Two-step BC (μg)
1	0.63	9	2.82	1	3.68	3.92	2.28
2	0.70	10	3.65	2	10.58	11.39	5.86
3	0.78	11	5.53	3	17.48	17.49	11.39
4	0.86	12	6.35	4	24.38	24.94	15.67
5	0.93	13	12.5	5	31.28	32.52	18.07
6	1.33	14	19.00	6	38.18	39.14	24.29
7	2.12	15	38.6	7	45.08	49.18	28.61
8	2.49	-	-	-	-	-	

带格式表格

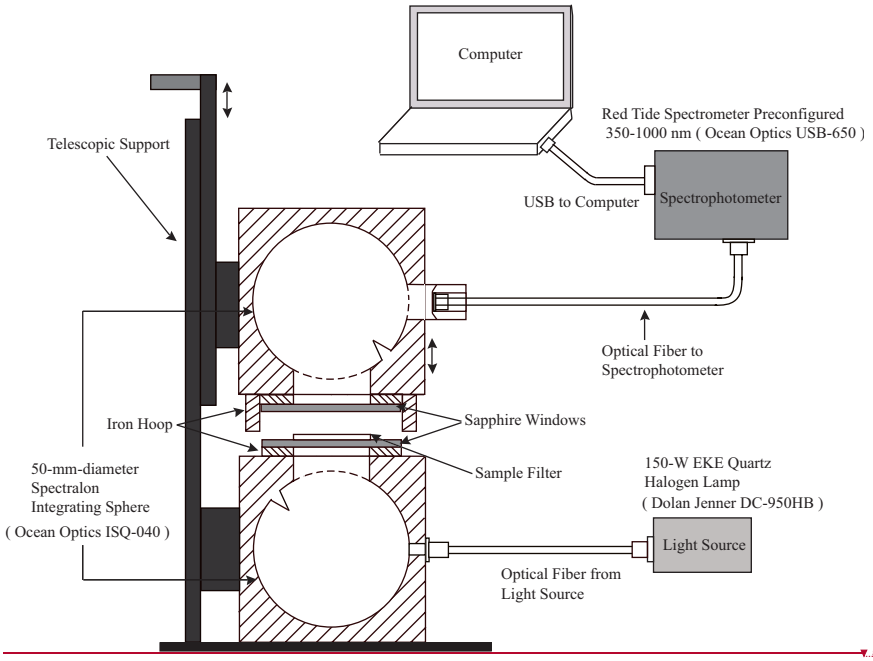

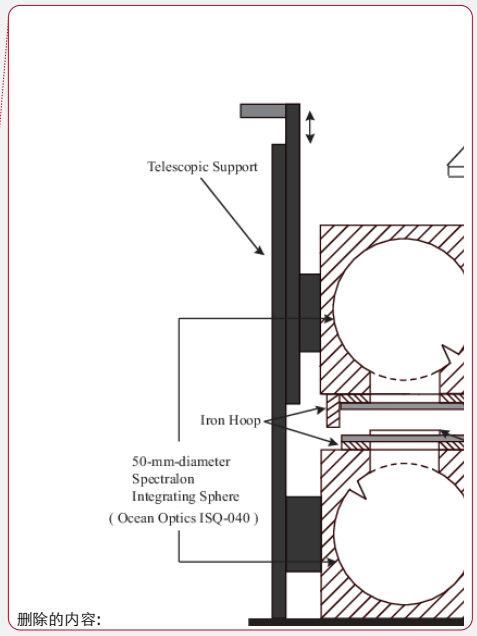

Figure 2 Schematic diagram of the improved two-sphere integrating spectrophotometer.

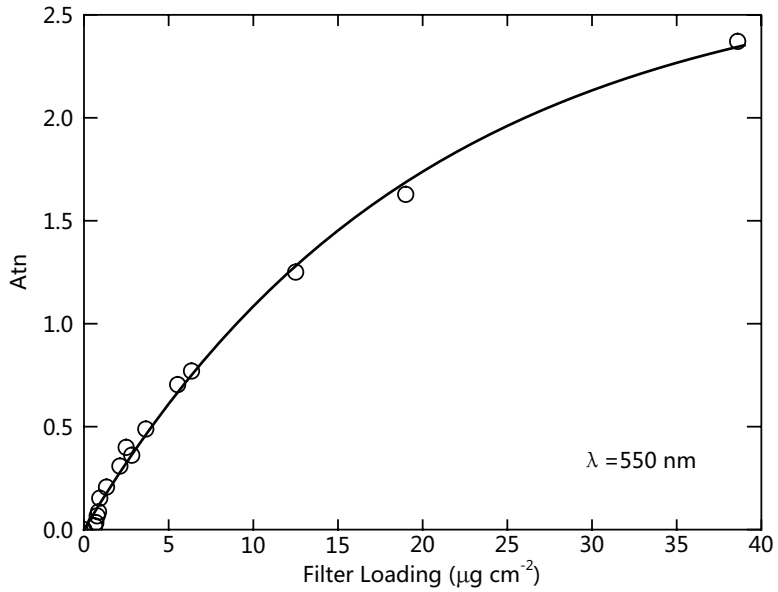

删除的内容:

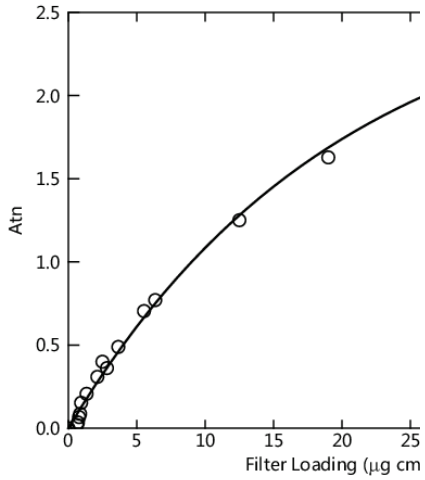

Figure 3 Calibration curve for standard fullerene soot at a wavelength of 550 nm. The solid line is a best-fit curve for the filter measurements. S_0 and S are the detected signals for the blank and sample filters, respectively, and $-\ln(S/S_0)$ is the relative attenuation.

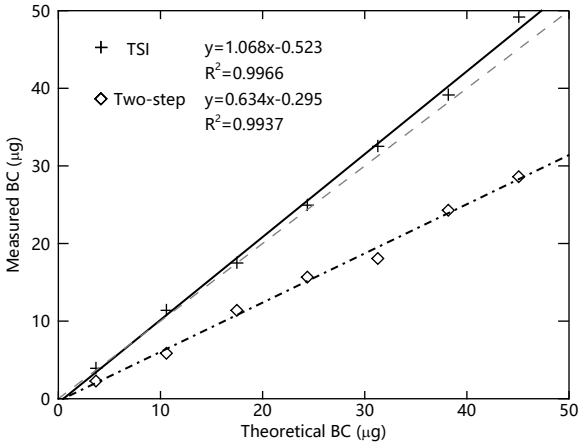

Figure 4 Comparison of the theoretical and measured BC mass determined by the TSI and two-step techniques in the laboratory. The solid and dot–dashed lines represent best-fit lines for the TSI and two-step techniques, respectively. The dashed line is a 1:1 line.

948
949
950
951
952
953

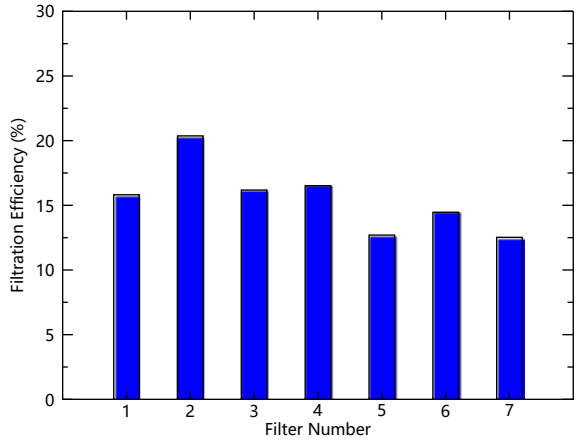

954

955 **Figure 5** Mass loss of standard fullerene soot on 1.0-μm quartz fiber filters determined
956 by refiltration using 0.4-μm Nuclepore filters.

957

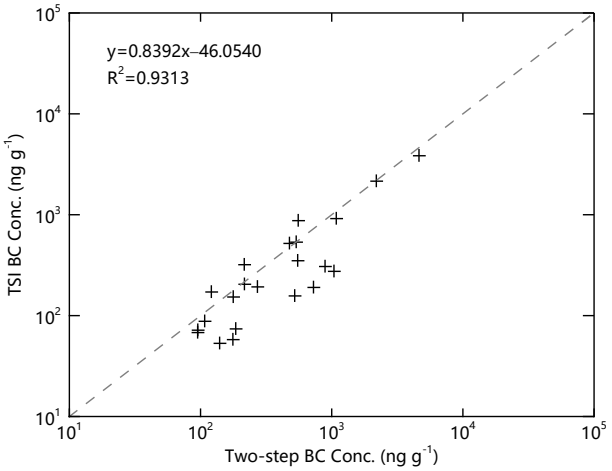

Figure 6 Comparison of BC concentrations in snow samples over northeast China during January–February 2014 determined by the TSI and two-step thermal optical methods. A 1:1 line (dashed) and a linear regression fit passing through the origin (solid curve) are also shown.

967
968
969
970
971

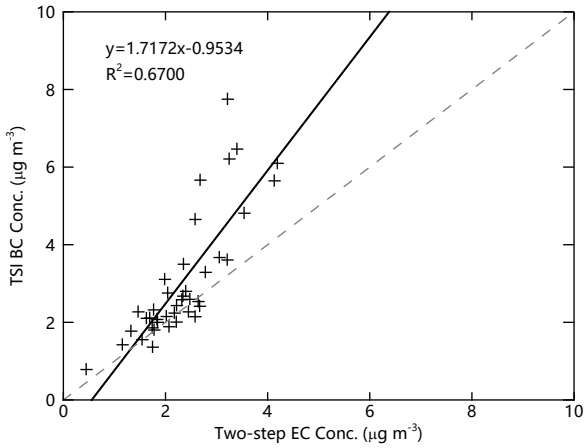

972

973 **Figure 7** As for Fig. 6, but for atmospheric samples collected at Lanzhou in northwest
974 China during 5–25 August 2015.

975

976 **Table 2** Statistics of BC and EC concentrations measured using the TSI and two-step
977 thermal–optical methods for snow samples during the experiments over northern China.
978

Site	Filter	TSI BC	Two-step EC
		ng g^{-1}	ng g^{-1}
90	Q-351L	349.95	550.19
91	Q-352L	171.46	120.87
	Q-352R	152.94	177.48
92	Q-354L	53.10	139.78
	Q-354R	57.82	176.41
93	Q-356L	71.71	95.27
	Q-356R	73.85	185.45
94	Q-358L	274.62	1040.20
95	Q-359L	87.84	107.51
	Q-359R	67.92	95.01
96	Q-363L	319.71	215.42
	Q-363R	192.60	271.42
97	Q-366L	204.47	216.04
	Q-366R	306.75	889.54
98	Q-369L	1605.95	130.36
	Q-369R	1321.69	6004.33
99	Q-376L	873.58	555.39
	Q-376R	534.70	536.11
100	Q-380R	519.47	476.14
101	Q-384R	3843.15	4626.72
102	Q-388L	915.59	1083.24
	Q-388R	2151.18	2187.90
103	Q-397L	156.76	522.07
	Q-397R	190.24	726.08

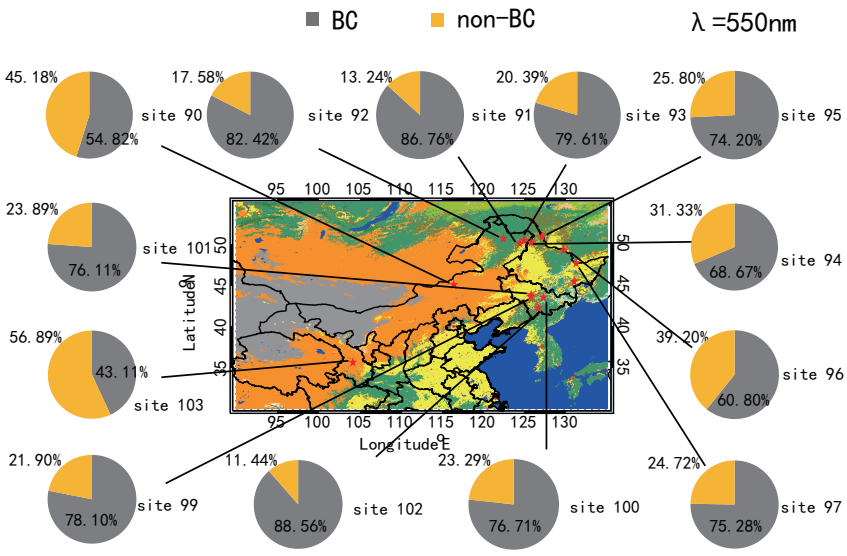

删除的内容:

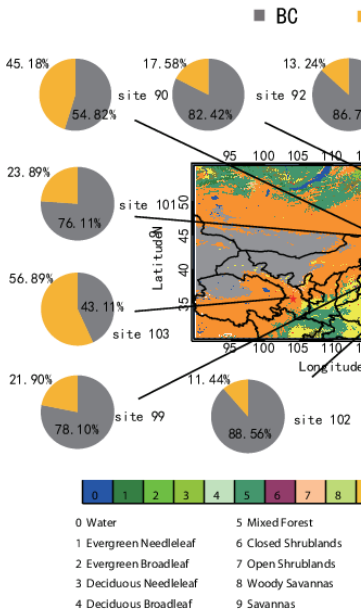

Figure 8 Spatial distributions of light absorption at 550 nm due to BC and non-BC fractions in surface snow across northern China during January–February 2014.

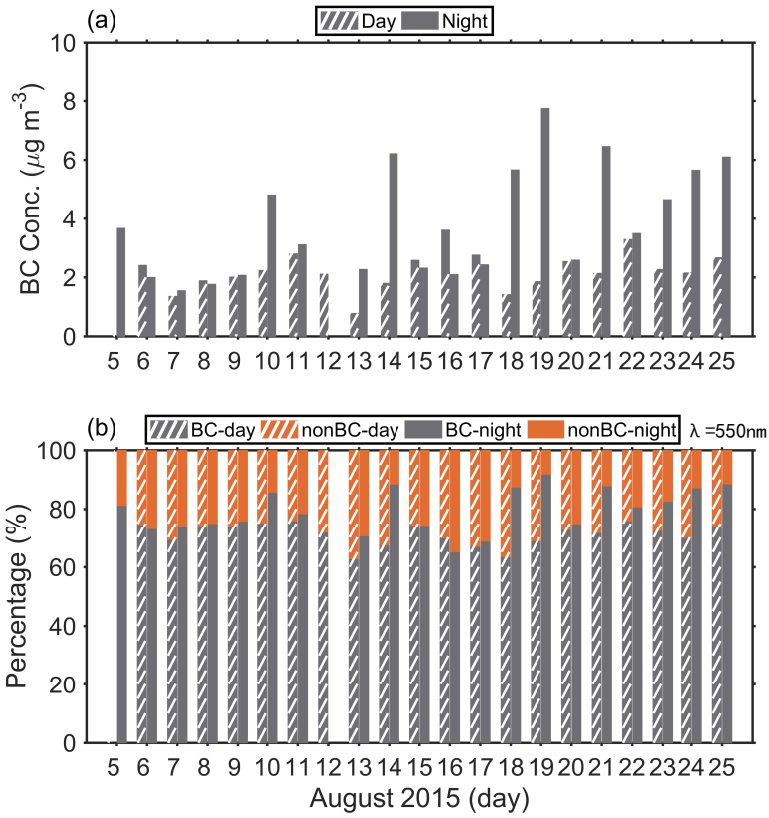

Figure 9 Variations in 8-hour **(a)** BC concentration and **(b)** BC and non-BC light absorption measured by TSI spectrophotometer at 550 nm at Lanzhou during 5–25 August 2015 (day: 9 am to 5 pm; night: 11 pm to 7 am).

带格式的: 居中

删除的内容:

994

995 **Table 3** Statistics of BC and EC concentrations in atmospheric samples measured using
996 the TSI and two-step thermal–optical methods.

Day			Night		
Date	TSI BC	Two-step EC	Date	TSI BC	Two-step EC
	μg m^{-3}	μg m^{-3}		μg m^{-3}	μg m^{-3}
2015. 8. 6	2. 41	2. 67	2015. 8. 5–8. 6	3. 67	3. 05
2015. 8. 7	1. 36	1. 75	2015. 8. 6–8. 7	2. 00	1. 84
2015. 8. 8	1. 89	2. 07	2015. 8. 7–8. 8	1. 55	1. 54
2015. 8. 9	2. 01	2. 21	2015. 8. 8–8. 9	1. 77	1. 32
2015. 8. 10	2. 24	2. 17	2015. 8. 9–8. 10	2. 07	1. 83
2015. 8. 11	2. 80	2. 40	2015. 8. 10–8. 11	4. 81	3. 54
2015. 8. 12	2. 11	1. 69	2015. 8. 11–8. 12	3. 11	1. 98
2015. 8. 13	0. 78	0. 45	2015. 8. 13–8. 14	2. 27	1. 46
2015. 8. 14	1. 80	1. 78	2015. 8. 14–8. 15	6. 21	3. 25
2015. 8. 15	2. 58	2. 32	2015. 8. 15–8. 16	2. 32	1. 77
2015. 8. 16	3. 61	3. 21	2015. 8. 16–8. 17	2. 10	1. 63
2015. 8. 17	2. 76	2. 04	2015. 8. 17–8. 18	2. 43	2. 22
2015. 8. 18	1. 42	1. 15	2015. 8. 18–8. 19	5. 66	2. 68
2015. 8. 19	1. 86	1. 74	2015. 8. 19–8. 20	7. 75	3. 21
2015. 8. 20	2. 54	2. 64	2015. 8. 20–8. 21	2. 59	2. 48
2015. 8. 21	2. 14	2. 58	2015. 8. 21–8. 22	6. 46	3. 40
2015. 8. 22	3. 29	2. 78	2015. 8. 22–8. 23	3. 50	2. 35
2015. 8. 23	2. 27	2. 45	2015. 8. 23–8. 24	4. 65	2. 58
2015. 8. 24	2. 15	2. 02	2015. 8. 24–8. 25	5. 65	4. 13
2015. 8. 25	2. 67	2. 34	2015. 8. 25–8. 26	6. 10	4. 19

997

998

Development of an improved two-sphere integration technique for quantifying black carbon concentrations in the atmosphere and seasonal snow

Xin Wang [1, 2], **Xueying Zhang** [3] and Wenjing Di [1]

[1] Key Laboratory for Semi-Arid Climate Change of the Ministry of Education, Lanzhou University, Lanzhou 730000, Gansu, China

[2] Institute of Surface-Earth System Science, Tianjin University, Tianjin 300072

[3] Jilin Weather Modification Office, Changchun 132000, Jilin, China

Correspondence to: Xin Wang (Tel: +86 931 8915892)

E-mail address: wxin@lzu.edu.cn (X. Wang)

Submitted on August 2019

Abstract. An improved two-sphere integration (TSI) technique has been developed to quantify black carbon (BC) concentrations in the atmosphere and seasonal snow. The major advantage of this system is that it combines two distinct integrated-spheres to reduce the scattering effect due to light-absorbing particles, and thus provides accurate determinations of total light absorption from BC collected on Nuclepore filters. The TSI technique can be calibrated using a series of 15 filter samples of standard fullerene soot. This technique quantifies the mass of BC by separating the spectrally resolved total light absorption into BC and non-BC fractions. To assess the accuracy of the improved system, an empirical procedure for measuring BC concentrations by a two-step thermal–optical method is also applied. Laboratory results indicate that BC concentrations determined using the TSI technique and theoretical calculations are well correlated (R^2=0.99), whereas the thermal–optical method underestimates BC concentrations by 35%–45% than that measured by TSI technique. Assessments of the two methods for atmospheric and snow samples revealed excellent agreement, with least-squares regression lines with slopes of 1.72 (r^2 = 0.67) and 0.84 (r^2 = 0.93), respectively. However, the TSI technique is more accurate in quantifications of BC concentrations in both the atmosphere and seasonal snow, with an overall lower uncertainty. Using the improved TSI technique, we find that light absorption at a wavelength of 550 nm due to BC plays a dominant role, relative to non-BC light absorption, in both the atmosphere (62.76%–91.84% of total light absorption) and seasonal snow (43.11%–88.56%) over northern China.

ARTICLE INFO

Keywords:

Black carbon

Elemental carbon

Light absorption

Two-sphere integration technique

Thermal–optical method

1 Introduction

Black carbon (BC) has long been recognized as the major light-absorbing particles (LAPs) in both natural and anthropogenic emissions (Slater et al., 2002; Koch et al., 2009; Zhang et al., 2009; Pan et al., 2010; McMeeking et al., 2011; Pavese et al., 2012; Bond et al., 2013; IPCC, 2013). BC can impact the regional and global climate in several ways, including via the direct effects of scattering and absorbing visible solar radiation (Jacobson, 2001b; Menon et al., 2002; Hansen et al., 2005; Ramanathan and Carmichael, 2008), the semi-direct effects of changing the temperature structure and relative humidity of the atmosphere by absorbing solar short-wave radiation (Weiss et al., 2012), and indirect effects on cloud formation and lifetime (Chuang et al., 2002; Baumgardner et al., 2004; Rosenfeld et al., 2008). Once deposited onto snow or ice surfaces, BC absorbs more solar radiation than pure snow or ice and reduces the snow albedo, thus accelerating snow melt (Xu et al., 2009a; Flanner et al., 2012; Hadley and Kirchstetter, 2012; Carmagnola et al., 2013; Qian et al., 2014; Zhao et al., 2014).

Optically classified BC is also often referred to as elemental carbon (EC), which is typically thermally detected. The distinction between BC and EC has been debated since the 1980s (Heintzenberg, 1989; Horvath, 1993a; Andreae and Gelencser, 2006; Moosmuller et al., 2009). Given that BC and EC are both soot particles with diameters of <1 μm, these terms have often been used interchangeably (Chow et al., 2001, 2004; Ming et al., 2009; Thevenon et al., 2009; Lim et al., 2014). BC is generally regarded as ideal light-absorbing particles of carbon, and is typically measured using optical attenuation methods (Clarke et al., 1987; Grenfell et al., 2011; Hansen et al., 1984; Ogren and Charlson, 1983). The term 'EC' is often used interchangeably with 'BC' when referring to optical absorption measurements (Clarke et al., 1987; Grenfell et al., 2011), and is only uniquely identified by thermal–optical methods (Xu et al., 2006; Cao et al., 2007; Jimenez et al., 2009). There remains poor agreement between measurements of BC and EC among available measurement techniques. The general techniques used to quantify the various fractions of BC mass concentrations are associated with the corresponding methods: thermal–optical methods, single-particle soot photometer (SP2) measurements, and filter-based optical techniques. Besides the above techniques, the aerosol mass spectrometry, electron

microscopy, and Raman spectroscopy are also useful and accurate methods to identify the various fractions of carbonaceous aerosols in the atmosphere (Cross et al., 2010; Ivleva et al., 2007; Spencer et al., 2007; Li et al., 2016; Petzold et al., 2013). Among these methods, the thermal–optical approach is regarded as the most effective and reliable for evaluating EC concentrations (Chylek et al., 1987; Cachier and Pertuisot, 1994; Jenk et al., 2006; Legrand et al., 2007; Hadley et al., 2010). However, the thermal–optical method can lead to large discrepancies in determining EC concentrations as a result of inference from positive artifacts caused by inadequately separated organics and mineral dust (Ballach et al., 2001; Wang et al., 2012). Further discrepancies are caused by the use of two main detection protocols [thermal–optical transmission (TOT) and thermal–optical reflectance (TOR)] to assess EC and OC concentrations based on their unique thermal properties. These protocols yield different OC and EC concentrations (Chow et al., 1993, 2001; Birch and Cary, 1996; Watson and Chow, 2002). The Integrating Sphere/Integrating Sandwich Spectrophotometer (ISSW) method was developed by Grenfell et al. (2011) and has been used to analyze mass concentrations of BC in snow (Doherty et al., 2010, 2014; Wang et al., 2013). Doherty et al. (2010) noted that the total uncertainty in measuring BC in snow using the ISSW method is up to 40% relative to the gravimetric standards of BC (fullerene soot). The total uncertainty associated with the filter-based ISSW technique on BC concentration determination for ambient snow has previously been estimated as 40 %, which is the sum, in quadrature, of 11% for instrumental uncertainty, 15% for undercatch uncertainty (loss of insoluble light-absorbing impurities), 17% for BC mass absorption coefficient (MAC) uncertainty, and 30% for uncertainty in the AAE of non-BC material (Doherty et al., 2010; Grenfell et al., 2011; Schwarz et al., 2012). Finally, the SP2 technique is well suited to the quantification of low BC concentrations with small particle radius (<500 nm). It is an optimized method for measuring BC concentrations and size distributions, and the substantially larger uncertainty of the SP2 instrument with respect to BC concentration measurements can exceed 60% in snow and ice cores, and 30% for atmospheric sampling (Schwarz et al., 2012). They noted that the relative transmission efficiencies of polystyrene latex sphere concentration standards (PSLs) in liquid to the SP2 after aerosolization remarkably reduce to 20% due to larger diameter of BC particles (>

500 nm). Therefore, the larger diameter of BC (>500 nm) is hardly captured by SP2 instrument with a collison-type nebulizer. Moreover, the mixing status of BC in snow is more complicated than the standard fullerene soot in the laboratory and the typical BC in the atmosphere.

Although several field campaigns have collected atmospheric, snow, and ice core samples to measure BC and EC concentrations globally (Wolff and Cachier, 1998; von Schneidemesser et al., 2009; Doherty et al., 2010, 2014; Ming et al., 2010; Huang et al., 2011; Xu et al., 2012; Cong et al., 2015), biases remain in determinations of BC concentrations, as is evident from a comparison among the results obtained with the SP2, ISSW, and thermal–optical methods (Schwarz et al., 2012; Lim et al., 2014). As a result, it is difficult to assess the effects of BC and EC on recent climate change using different techniques, even in the same area.

Here we report the development of a new portable and accurate spectrophotometric method based on the two-sphere integration (TSI) technique that can be used to determine BC concentrations in both the atmosphere and seasonal snow. The improved TSI technique minimizes scattering effects related to BC and non-BC insoluble particles collected on Nuclepore filters, and thus provides a simple and accurate means to assess BC concentrations in the atmosphere and seasonal snow. To assess the accuracy of the new technique, a two-step thermal–optical method is applied to determine BC concentrations on individual quartz fiber filters. Finally, we investigate the spatial distribution of BC concentrations and the relative light absorption of surface snow over northeast China. We also analyze the diurnal variations of BC in the atmosphere during day and night over Lanzhou in northwest China.

2 Experimental Procedures

2.1 Sampling sites and snow-sample filtration

During the study period, less snow fell in 2014 than in 2010, and no seasonal snow was present in the western part of Inner Mongolia. Therefore, we collected 94 snow samples at 14 sites in January and February of 2014 across north China following the sampling route

of Huang et al. (2011). The sites are numbered in chronological order from 90 to 103, following previous snow surveys (Ye et al., 2012; Wang et al., 2013). Figure 1 shows the locations of the snow field campaigns across northern China. The sampling locations were selected to be at least 50 km from any settlement and 1 km from the nearest road. Snow samples were kept frozen before being filtered. We set up a temporary laboratory along the sampling route. Owing to BC in snow is often hydrophobic, long time melting could lose more BC to the container walls instead of collected on the filter (Ogren et al., 1983). In order to minimize the loss of insoluble ILAPs, we quickly melted the snow samples in a microwave within a very short time. Therefore, the loss of insoluble LAPs is very limited, and can be neglectable. At present, this method is widely performed for snow melting procedure. (Dothery et al., 2010, 2014; Wang et al.,2013). Subsequently, we simultaneously filtered the snow samples using quartz fiber filters with 1-μm pores and Nuclepore filters with 0.4-μm pores. Then, we refiltered the snow samples for the quartz fiber filters using Nuclepore filters with 0.4-μm pores to account for the loss of BC mass in the 1-μm pore quartz fiber filters. Finally, we stored the original and refiltered snow samples in clean high-density polyethylene bottles in a freezer at −30°C for subsequent analysis. For details of the sampling and filtration procedures, see Wang et al. (2013).

To evaluate the accuracy of the TSI technique in measuring BC concentrations, the atmospheric samples were collected continuously on Nuclepore and quartz fiber filters with high-volume samplers during the periods 09:00 to 17:00 (daytime; local time) and 23:00 to 07:00 (nighttime) at site 103 in Lanzhou from 5 to 25 August 2015. The pumps were operated at a flow rate of 10 L min^{-1}. In total, 40 atmospheric samples were collected during this experiment and used to assess the accuracy of the atmospheric BC concentration measurements of the improved TSI technique.

2.2 Two-sphere integration technique

Light transmission techniques are the most commonly used methods for determining light-absorbing impurities in aerosol filter samples of the atmosphere and snow/ice. Since the 1970s, a series of optical attenuation techniques have been developed for estimating BC concentrations using light transmission changes through filters, based on Beer's law. An integrating sphere (IS) technique was first proposed for measuring BC by Fischer

(1970). The integrating sphere was coated with diffusely reflecting white paint through a small hole, and the reduction in signal after measuring the sample filters represented the absorption of BC. Subsequently, a new integrating plate (IP) instrument was developed to measure scavenging BC on filters based on the IS technique, which uses a light-diffusing support to provide a nearly Lambertian light source for light transmission using 0.4-μm Nuclepore filters (Clarke et al., 1987; Horvath, 1993b). However, the multiple scattering of solar radiation affect the accuracy of the IP technique (Clarke et al., 1987; Hitzenberger, 1993; Petzold et al., 1997; Bond et al., 1999). A new integrating-sandwich configuration of the ISSW instrument was designed to measure the absorption of light-absorbing impurities based on the ISSW principle of Grenfell et al. (2011). The ISSW instrument can isolate the absorption properties of light-absorbing impurities deposited on polycarbonate Nuclepore filters. By assuming the mass absorption efficiency and non-BC Ångström exponent at 550 nm, this technique is currently capable of reliably measuring BC and non-BC light absorption (Wang et al., 2013; Dang and Hegg, 2014; Doherty et al., 2014). However, Schwarz et al. (2012) found that the total instrumental uncertainty associated with ISSW BC concentration determinations for ambient snow is 11%, and that this uncertainty is partially due to the scattering effects of insoluble impurities deposited on the filters (Doherty et al., 2010; Grenfell et al., 2011).

The improved TSI spectrophotometer developed in this study is small, lightweight, and portable, and can accurately quantify BC concentrations using a technique based on the integrating sphere and integrating plate transmission techniques (Fig. 2). The major improvement of this spectrophotometer is that we replaced the integrating sandwich of the ISSW instrument developed by Grenfell et al. (2011) with a new integrating sphere. In addition, an iron hoop is applied to the top integrating sphere surrounding the sapphire windows to reduce light scattering due to insoluble particles on the filters. Therefore, the total relative light absorption due to all insoluble impurities on the filter can be estimated from the visible-to-near-infrared wavelengths. The total light attenuation can be calculated from the light transmitted by a snow or atmospheric sample, $S(\lambda)$, compared with that transmitted by a blank filter, $S_0(\lambda)$. Then, the relative attenuation (Atn) through the filter can be expressed as follows

$$Atn = -\ln[S(\lambda)/S_0(\lambda)] \quad (1)$$

Then, the total absorption Ångström exponent $\text{Å}_{tot}(\lambda_0)$ of all the ILAPs on the filters can be calculated from the following formula:

$$\text{Å}_{tot}(\lambda_0) = -\frac{\ln[\tau_{tot}(\lambda_1)/\tau_{tot}(\lambda_2)]}{\ln(\lambda_1/\lambda_2)} \quad (2)$$

Å_{non-BC} is calculated as a linear combination of the contributions to light absorption made by OC and Fe:

$$\text{Å}_{non-BC} = \text{Å}_{OC} \times f_{OC} + \text{Å}_{Fe} \times f_{Fe} \quad (3)$$

The total absorption Ångström exponent of all ILAPs on a filter (Å_{tot}) can be described as a linear combination of Å_{BC} and Å_{non-BC} weighted by the light absorption fraction:

$$\text{Å}_{tot}(\lambda_0) = \text{Å}_{BC} \times f_{BC}(\lambda_0) + \text{Å}_{non-BC} \times f_{non-BC}(\lambda_0) \quad (4)$$

Using the mass absorption efficiency and absorption Ångström exponents for BC, OC, and Fe described by Wang et al. (2013), we can further estimate the following parameters: equivalent BC (C_{BC}^{equiv}), maximum BC (C_{BC}^{max}), estimated BC (C_{BC}^{est}), fraction of light absorption by non-BC ILAPs (insoluble light-absorbing particles) (f_{non-BC}^{est}), absorption Ångström exponent of non-BC ILAPs ($Å_{non\text{-}BC}$), and total absorption Ångström exponent ($Å_{tot}$). These parameters are defined as follows.

1. C_{BC}^{equiv} (ng g^{-1}): *equivalent BC* is the amount of BC that would be needed to produce the total light absorption by all insoluble particles in snow for wavelengths of 300–750 nm.
2. C_{BC}^{max} (ng g^{-1}): *maximum BC* is the maximum possible BC mixing ratio in snow, assuming that all light absorption is due to BC at wavelengths of 650–700 nm.
3. C_{BC}^{est} (ng g^{-1}): *estimated BC* is the estimated true mass of BC in snow derived by separating the spectrally resolved total light absorption and non-BC fractions.
4. f_{non-BC}^{est} (%): the *fraction of light absorption by non-BC light-absorbing particles* is the integrated absorption due to non-BC light-absorbing particles. This value is weighted by the down-welling solar flux at wavelengths of 300–750 nm.
5. $Å_{non\text{-}BC}$: the *non-BC absorption Ångström exponent* is derived from the light absorption by non-BC components for wavelengths of 450–600 nm.
6. $Å_{tot}$: the *absorption Ångström exponent* is calculated for all insoluble particles deposited on the filter between 450 and 600 nm.

Furthermore, combining with the mass loading of Fe was determined by chemical analysis (Wang et al., 2013), the mass loading of OC (L_{OC}) was also estimated assuming

that the MAC for OC is 0.3 m^2 g^{-1} at the wavelength of 550 nm using the following equation:

$$\tau_{tot}(\lambda) - MAC_{BC}(\lambda) \times L_{BC}^{est} - MAC_{Fe} \times L_{Fe} = MAC_{OC} \times L_{OC} \quad (5)$$

All relevant equations and associated derivations are described by Grenfell et al. (2011) and Doherty et al. (2010, 2014). Note that the calculation of non-BC light absorption due to insoluble impurities assumes that the iron in snow is predominantly from mineral dust (Wang et al., 2013).

2.3 Calibration of the TSI spectrophotometer

In this study, a series of 15 Nuclepore filters with a pore size of 0.2 μm (LOT# 7012284, 25mm, Whatman) loaded with fullerene soot (stock #40971, lot #L20W054, Alfa Aesar, Ward Hill, MA, USA) is used to calibrate the spectrophotometer over the range 0.63–38.6 μg, which typically covers >75% of ambient accumulation mode mass (left panel in Table 1; Schwarz et al., 2012). Fullerene soot is commonly used for calibrating the light transmission and thermal–optical techniques for measuring BC concentrations (Baumgardner et al., 2012). Standard fullerene soot particles are fractal-like aggregates of spherical primary particles with a diameter of ~50 nm, with a mean density of 1.05 g cm^{-3} (Moteki et al., 2009). Multiple filters with various loadings are required, as the system response deviates from Beer's law exponential behavior; related equations can be found in Grenfell et al. (2011). Note that uncertainties in mass absorption efficiencies, which range from 2 to 25 m^2 g^{-1}, can lead to uncertainty in this technique. Here, we use a mass absorption efficiency of 6.22 m^2 g^{-1} at 525 nm, which is consistent with Doherty et al. (2010) and Grenfell et al. (2011). Figure 3 shows the best-fit curve (solid line) of loading of the filters at 550 nm. When the filter loading was 0–40 μg cm^{-2}, all measured results were close to the best-fit curve, indicating that the TSI spectrophotometer is stable and accurate in terms of BC mass measurements.

2.4 Thermal–optical measurements of EC concentration

There are several types of thermal–optical method that can be used to quantify EC and OC concentrations, including two-step temperatures in oxidizing/non-oxidizing atmospheres (Cachier et al., 1989; Xu et al., 2006, 2009b), thermal–optical reflectance

(Chow et al., 1993, 2001; Chen et al., 2004), and thermal–optical transmittance (Sharma et al., 2002; Yang and Yu, 2002; Chow et al., 2004). Using an optimized two-step method, Cachier et al. (1989) first confirmed that soot carbon not only comprises EC, but is also mixed with highly condensed organic material. An optimized two-step thermal–optical system has been developed to detect EC and OC concentrations in ice cores (Xu et al., 2006). Here, we use the optimized two-step method based on the thermal–optical technique to measure EC concentrations. In this experiment, quartz fiber filters were first preheated in a muffle furnace at 350°C to remove organic carbon prior to sampling. All filters were punched to yield appropriately sized samples for analysis. Snow samples were analyzed for EC and OC concentrations using a Thermal–Optical Carbon Analyzer (Desert Research Institute, Model 2001A), following the thermal–optical reflectance (TOR) protocol of the Interagency Monitoring of Protected Visual Environments (IMPROVE_A). We developed a new method, referred to as the two-step method, to measure the concentrations of BC collected by the quartz fiber filters. The two-step method is an updated measurement procedure that first extracts an OC fraction below 550°C in a He atmosphere. The volatilized OC is oxidized to CO_2, reduced to CH_4, and detected by a flame ionization system. Next, two EC fractions (EC1 and EC2) are extracted above 550°C in an atmosphere of 2% O_2 and 98% He. Detailed procedures can be found in Xu et al. (2006) and Chow et al. (2004). The analytical uncertainty of this method is 15% for BC and 16% for OC measured via four parallel ice samples cut lengthways in an ice core with high dust loading (Xu et al., 2009a).

3 Results

3.1 Comparison with theoretical calculations

To further assess the accuracy of the TSI system, we use standard fullerene soot and quantify BC concentrations using theoretical calculations for comparison with BC values measured by a laboratory-based TSI spectrophotometer. To ensure the stability and accuracy of the improved TSI spectrophotometer, two individual sets of standard BC filters were used: 0.4-μm Nuclepore and 1-μm quartz fiber filters. All filters were preheated in a muffle furnace at 350°C to remove organic carbon prior to sampling. A measured amount

of BC was mixed into a known volume of ultrapure water. The mixture was then agitated by ultrasound for ~10 min, and the same volumes of liquid were then filtered through the two types of filter. Using the calculated BC mass, seven filters with gradually increasing BC concentrations were obtained for both the 0.4-μm Nuclepore and 1-μm quartz fiber filters. Next, all the filters were placed in a dryer for 24 h and then measured using the TSI spectrophotometer. Using the BC mass and the volume of the ultrapure water used for filtration, we can estimate the theoretical BC concentration for each filter. The mass for each filter is listed in Table 1 (right panel).

Assuming a mass absorption cross-section (MAC) of BC of 6.22 m^2 g^{-1} at 525 nm, the BC concentrations measured using the TSI spectrophotometer were in good agreement with the theoretical BC values in the slope of 1.07 (Figure 4). The BC mass loaded on the Nuclepore filters was approximately equal to that measured by the improved TSI spectrometer, which indicates that the TSI system developed here can accurately measure BC concentrations with the assumed mass absorption efficiency. In contrast, the standard BC mass on the quartz fiber filters was underestimated by 35%–45% using the two-step thermal–optical technique, compared with the theoretical value. During the filtration process, we found that the time required to filter liquid snow samples on the 0.4-μm Nuclepore filters was much longer than was the case for the 1-μm quartz fiber filters. Therefore, we first filtered the melted snow samples on the quartz fiber filters, and then re-filtered the snow samples using the 0.4-μm Nuclepore filters. Using this process, BC mass losses can be obtained using the TSI technique, assuming optical BC is equivalent to thermal EC.

As shown in Figure 5, the fraction of BC mass collected during the second filtration (0.4-μm filter) ranges from 12% to 21% of the total collected mass (filter directly with 0.4-μm filters), as might be expected for the small particles of standard fullerene soot (<50 nm). This under-sampled fraction decreases with increasing BC mass on the filters, possibly owing to blocking of the filter pores. As a result, the under-sampled fraction of the thermal–optical method was larger than that of the TSI technique, leading to a lower filtration efficiency. Note that these sampling efficiencies are strongly related to the BC size distribution. Therefore, the improved TSI technique developed here is more stable and accurate for measuring pure BC masses, and the data obtained using this method can be

used as the standard BC mass. After correcting for systematic biases, the results of both methods were closer to the theoretical BC calculations. Note, however, that the size distribution of the laboratory BC standard was much smaller than those of the atmospheric and seasonal snow samples (Schwarz et al., 2012). Therefore, underestimates caused by the filtration efficiency for ambient BC should be lower than that for the standard BC.

3.2 Comparison of BC concentrations in seasonal snow and the atmosphere

Recent studies have indicated that mineral dust can affect the accurate detection of BC concentrations using the ISSW and thermal–optical methods (Wang et al., 2012; Zhou et al., 2017). To eliminate the large uncertainty and bias due to dust particles, we only used snow samples collected in industrial areas over northeastern China, where the light absorption was dominated by fine-mode ILAPs (e.g., BC and OC; Wang et al., 2013). Hence, most of the snow samples did not contain very large coarse-mode particles, such as mineral and local soil dust.

During the snow field campaign, two series of snow samples were filtered through the Nuclepore and quartz fiber filters and measured using the TSI and two-step thermal–optical methods (Fig. 6). Result shows that most of the BC values measured by the TSI and two-step thermal–optical methods are close to the 1:1 line in a comparison plot, and are generally in good agreement (slope of 1.11, $R^2 = 0.93$, n = 22). However, some BC values in seasonal snow measured by the two-step thermal–optical method are much larger than those measured by the TSI technique. Consequently, for each sample the mean ratio of BC concentrations measured by the two-step method and the TSI spectrophotometer varies from 0.64 to 3.97, with an overall mean of 1.57. This discrepancy arises from two factors. First, Wang et al. (2017) found that snow grain sizes varied considerably (from 0.07 to 1.3 mm) during this snow field campaign. This range is much larger than that recorded in previous studies, owing to snow melting by solar radiation and ILAPs (Hadley and Kirchstetter, 2012; Painter et al., 2013; Yasunari et al., 2013; Pedersen et al., 2015). These results agree well with those of Schwarz et al. (2012), who found that the sizes of BC particles in snow are much larger than those in typical ambient air. Therefore, the sampling efficiency of the quartz fiber filters could have been significantly higher than expected. The other factor is that the insoluble light-absorbing impurities in seasonal snow over

northeast China contained not only BC, but also insoluble organic carbon. This result is consistent with a previous study by Chow et al. (2004), who reported that the charring observed when employing the two-step thermal–optical method at higher temperatures (>550°C) was incomplete and that certain organic compounds are not completely pyrolyzed below 550°C. Therefore, incomplete charring of absorbed organic compounds by the two-step processes may lead to incompletely pyrolyzed OC on the filters, artificially contributing to the BC concentration. This may explain why the BC concentration measured using the thermal–optical method was higher than that measured using the TSI spectrophotometer.

A comparison of BC concentrations in the atmosphere measured by the ISSW and thermal–optical methods is vastly different than that for the snow samples (Fig. 7). Results are in excellent agreement for BC concentrations of <3 μg m^{-3}. However, biases increased gradually with increasing BC concentrations, leading to two-step-to-TSI ratios as low as 0.5. The BC concentrations of >3 μg m^{-3} obtained using the two-step thermal–optical method are much lower than those measured using the improved TSI technique, possibly due to the small particle sizes in the atmosphere, which lead to a lower filtration efficiency. Overall, we conclude that the improved TSI method is more stable and suitable for measuring BC concentrations in both the atmosphere and snow samples compared with the two-step thermal–optical method.

3.3 Spatial distribution of BC and non-BC light absorption measured by the TSI spectrophotometer

The above results show that the improved TSI method measures BC concentrations in the atmosphere and snow/ice with higher accuracy than Two-step thermal optical methods. In this section we investigate the spatial distribution of BC concentrations and their relative light absorption due to BC and non-BC snow impurities in seasonal snow over northeast China during January–February 2014. All BC mass concentrations in surface snow measured by the TSI and thermal–optical methods during the snow field campaigns are listed in Table 2. There was less snow fall in January 2014 than in 2010, and seasonal snow did not cover all of central Inner Mongolia during this time. Thus, we only collected snow

samples at site 90. Given that this region is windy, the surface snow collected included drifted and aged snow. The surface BC concentration was 350 ng g^{-1} in the central Inner Mongolia region. The lowest BC concentrations in surface snow, 55 and 280 ng g^{-1}, were found on the border of northeast China (sites 91–97). We note that there were considerable variations in BC concentrations in these regions. The median BC concentration was 1100 ng g^{-1} with a range of 520–3900 ng g^{-1} for surface snow in northeast industrial regions. On 10 February 2014, fresh snow samples were collected in Lanzhou, at a mean snow depth of 6–8 cm. The mean BC concentration in these fresh snow samples from Lanzhou was ~170 ng g^{-1}.

The relative light absorption due to BC and non-BC fractions in seasonal snow measured using the improved TSI technique across northern China is shown in Figure 8. A similar pattern for the light absorption of BC (~70%) and non-BC (~30%) from insoluble light-absorbing impurities in surface snow indicates a similar pollution emission source over northeast China. However, the light absorption due to BC in seasonal snow plays a dominant role (43.11%–88.56%, with a mean of 73.10%). The largest BC light absorption was at site 102. This site is located in the central part of Jilin province, which is polluted by heavy industrial activity. For one sample, the light absorption of non-BC impurities in seasonal snow reached 56.89%, which is the only time it exceeded BC light-absorption. Biomass burning and fossil fuel are likely the major emission sources during the winter in Lanzhou, unlike the case over northeast China. These results are consistent with those of Wang et al. (2013), who found that snow particle light absorption was dominated by BC in northeast China in 2010.

Finally, we investigate atmospheric BC mass concentrations and their relative light absorption measured by the TSI spectrophotometer in Lanzhou during 5–25 August 2015. During this experiment, there were no noticeable trends of BC concentrations in Lanzhou. However, a notable feature in Figure 9 is that the BC mass concentrations at night are generally much higher than during the day (Table 3). The unique topography of Lanzhou likely plays an important role in this phenomenon. Lanzhou is situated in a valley basin with low rainfall, high evaporation, low wind speeds, and high calm-wind frequency, which often leads to a thick inversion layer in which air pollutants accumulate during the

night. The light absorption due to BC in the atmosphere ranges from 62.76% to 91.84%, with a mean of 75.43%.

4 Conclusions

We developed an improved two-sphere integration (TSI) spectrophotometer to quantify BC concentrations in snow and atmospheric samples over northern China. The TSI technique significantly reduces scattering effects caused by insoluble impurities deposited on filters. Therefore, the system more accurately measures light absorption due to BC and non-BC impurities. A system calibration using theoretical calculations for standard fullerene soot revealed that the TSI system can be used to assess BC concentrations with low uncertainty. A laboratory comparison revealed that the thermal–optical method can lead to a significant underestimate (35%–45%) of BC concentrations for small-diameter particles (~50 nm) due to the low filtration efficiency of 1-μm quartz fiber filters.

To further assess the accuracy of the improved TSI system, two field campaigns were carried out to collect seasonal snow and atmospheric samples during January–February 2014 and 5–25 August 2015 across northern China, respectively. Although the BC concentrations measured by the TSI and thermal–optical methods are well correlated for both the snow and atmospheric samples, we find that some BC values in seasonal snow measured by the two-step thermal–optical method were significantly overestimated compared with those measured by the TSI technique, by a factor of 1.57. Overall, the improved TSI optical system developed here is applicable to quantifications of BC concentrations in the atmosphere and snow/ice.

The spatial distribution of BC concentrations in seasonal snow over northern China during January–February 2014 ranged from 60 to 3800 ng g^{-1}, with a mean value of 700 ng g^{-1}, and ranged from 0.78 to 7.75 μg m^{-3} in the atmosphere during 5–25 August 2015 in Lanzhou. The spatial distribution of BC concentrations shows that large BC values are found mainly in the center of industrial regions near the central part, whereas lower values are found in northeast China. Light absorption is dominated by BC (~40% to 90%) in seasonal snow over northeast China, and this plays a dominant role in accelerating snow melt. Atmospheric samples collected in Lanzhou show significant changes in BC concentrations between day and night. Frequent, stable atmospheric boundary layers at

night during summer, caused by the valley-basin topography of Lanzhou, are largely responsible for air pollutant accumulation during the night.

Data availability. Data used in this paper are available upon request from corresponding author (wxin@lzu.edu.cn).

Author contributions. The conceptualization and methodology were done by XW. The experiments were designed by XZ and WD. The formal analysis, investigation, writing of the original draft, and editing were performed by XW.

Competing interests. The authors declare that they have no conflict of interest.

Acknowledgements. We thank Thomas C. Grenfell and Qiang Fu from University of Washington for providing the standard filters.

Financial support. This research was supported jointly by the National Key R&D Program of China (2019YFA0606801), the National Natural Science Foundation of China (41975157, 41775144, 41675065, and 41875091), and the Fundamental Research Funds for the Central Universities (lzujbky-2018-k02).

References

Andreae, M.O. and Gelencser, A.: Black carbon or brown carbon? The nature of light-absorbing carbonaceous aerosols, Atmos. Chem. Phys., 6, 3131-3148, doi: 10.5194/acp-6-3131-2006, 2006.

463 Ban-Weiss, G.A., Cao, L., Bala, G., and Caldeira, K.: Dependence of climate forcing and
464 response on the altitude of black carbon aerosols, Clim. Dyn., 38, 897-911, doi:
465 10.1007/s00382-011-1052-y, 2012.
466 Ballach, J., Hitzenberger, R., Schultz, E., and Jaeschke, W.: Development of an improved
467 optical transmission technique for black carbon (BC) analysis, Atmos. Environ. , 35,
468 2089-2100, doi: 10.1016/S1352-2310(00)00499-4, 2001.
469 Baumgardner, D., Kok, G., and Raga, G.: Warming of the Arctic lower stratosphere by
470 light absorbing particles, Geophys. Res. Lett., 31, doi: 10.1029/2003GL018883,
471 2004.
472 Baumgardner, D., Popovicheva, O., Allan, J., Bernardoni, V., Cao, J., Cavalli, F., Cozic, J.,
473 Diapouli, E., Eleftheriadis, K., Genberg, P.J., Gonzalez, C., Gysel, M., John, A.,
474 Kirchstetter, T.W., Kuhlbusch, T.A.J., Laborde, M., Lack, D., Muller, T., Niessner, R.,
475 Petzold, A., Piazzalunga, A., Putaud, J.P., Schwarz, J., Sheridan, P., Subramanian, R.,
476 Swietlicki, E., Valli, G., Vecchi, R., and Viana, M.: Soot reference materials for
477 instrument calibration and intercomparisons: a workshop summary with
478 recommendations, Atmos. Meas. Tech., 5, 1869-1887, doi: 10.5194/amt-5-1869-
479 2012, 2012.
480 Birch, M.E.: Analysis of carbonaceous aerosols: interlaboratory comparison, Analyst
481 123, 851-857, doi: 10.1039/A800028J, 1998.
482 Birch, M. E., and Cary, R. A.: Elemental carbon-based method for monitoring
483 occupational exposures to particulate diesel exhaust, Aerosol Sci. Technol., 25, 221-
484 241, doi: 10.1080/02786829608965393, 1996.
485 Bond, T.C., Bussemer, M., Wehner, B., Keller, S., Charlson, R.J., and Heintzenberg, J.:
486 Light absorption by primary particle emissions from a lignite burning plant,
487 Environ. Sci. Technol., 33, 3887-3891, doi: 10.1021/es9810538, 1999.
488 Bond, T.C., Streets, D.G., Yarber, K.F., Nelson, S.M., Woo, J.H., and Klimont, Z.: A
489 technology-based global inventory of black and organic carbon emissions from
490 combustion, J. Geophys. Res.-Atmos., 109, doi:10.1029/2003JD003697, 2004.
491 Bond, T.C., Doherty, S.J., Fahey, D.W., Forster, P.M., Berntsen, T., DeAngelo, B.J., Flanner,
492 M.G., Ghan, S., Karcher, B., Koch, D., Kinne, S., Kondo, Y., Quinn, P.K., Sarofim, M.C.,

493 Schultz, M.G., Schulz, M., Venkataraman, C., Zhang, H., Zhang, S., Bellouin, N.,
494 Guttikunda, S.K., Hopke, P.K., Jacobson, M.Z., Kaiser, J.W., Klimont, Z., Lohmann, U.,
495 Schwarz, J.P., Shindell, D., Storelvmo, T., Warren, S.G., and Zender, C.S.: Bounding
496 the role of black carbon in the climate system: A scientific assessment, J. Geophys.
497 Res.-Atmos., 118, 5380-5552, doi: 10.1002/jgrd.50171, 2013.
498 Cachier, H., Bremond, M.P., and Buat-Menard, P.: Determination of atmospheric soot
499 carbon with a simple thermal method, Tellus B., 41, 379-390, doi: 10.1111/j.1600-
500 0889.1989.tb00316.x , 1989.
501 Cachier, H. and Pertuisot, M.H.: Particulate Carbon in Arctic Ice, Analusis, 22, M34-
502 M37, 1994.
503 Cao, J.J., Lee, S.C., Ho, K.F., Zhang, X.Y., Zou, S.C., Fung, K., Chow, J.C., and Watson, J.G.:
504 Characteristics of carbonaceous aerosol in Pearl River Delta Region, China during
505 2001 winter period, Atmos. Environ., 37, 1451-1460, doi: 10.1016/S1352-
506 2310(02)01002-6, 2003.
507 Cao, J.J., Wu, F., Chow, J.C., Lee, S.C., Li, Y., Chen, S.W., An, Z.S., Fung, K.K., Watson, J.G.,
508 Zhu, C.S., and Liu, S.X.: Characterization and source apportionment of atmospheric
509 organic and elemental carbon during fall and winter of 2003 in Xi'an, China, Atmos.
510 Chem. Phys., 5, 3127-3137, doi: 10.5194/acp-5-3127-2005, 2005.
511 Cao, J.J., Lee, S.C., Chow, J.C., Watson, J.G., Ho, K.F., Zhang, R.J., Jin, Z.D., Shen, Z.X., Chen,
512 G.C., Kang, Y.M., Zou, S.C., Zhang, L.Z., Qi, S.H., Dai, M.H., Cheng, Y., and Hu, K.: Spatial
513 and seasonal distributions of carbonaceous aerosols over China, J. Geophys. Res.-
514 Atmos., 112, doi: 10.1029/2006JD008205, 2007.
515 Carmagnola, C.M., Domine, F., Dumont, M., Wright, P., Strellis, B., Bergin, M., Dibb, J.,
516 Picard, G., Libois, Q., Arnaud, L., and Morin, S.: Snow spectral albedo at Summit,
517 Greenland: measurements and numerical simulations based on physical and
518 chemical properties of the snowpack, The Cryosphere, 7, 1139-1160, doi:
519 10.5194/tc-7-1139-2013, 2013.
520 Chen, L.W.A., Chow, J.C., Watson, J.G., Moosmuller, H., and Arnott, W.P.: Modeling
521 reflectance and transmittance of quartz-fiber filter samples containing elemental

522 carbon particles: Implications for thermal/optical analysis, J. Aerosol Sci., 35, 765-
523 780, doi: 10.1016/j.jaerosci.2003.12.005, 2004.
524 Chow, J.C., Watson, J.G., Pritchett, L.C., Pierson, W.R., Frazier, C.A., and Purcell, R.G.:
525 The Dri Thermal Optical Reflectance Carbon Analysis System - Description,
526 Evaluation and Applications in United-States Air-Quality Studies, Atmos. Environ.,
527 27, 1185-1201, doi: 10.1016/0960-1686(93)90245-T , 1993.
528 Chow, J.C., Watson, J.G., Lu, Z.Q., Lowenthal, D.H., Frazier, C. A., Solomon, P. A., Thuillier,
529 R. H., Magliano, K.: Descriptive analysis of PM(2.5) and PM(10) at regionally
530 representative locations during SJVAQS/AUSPEX. Atmos. Environ., 30, 2079-2112,
531 doi: 10.1016/1352-2310(95)00402-5, 1996.
532 Chow, J.C., Watson, J.G., Crow, D., Lowenthal, D.H., and Merrifield, T.: Comparison of
533 IMPROVE and NIOSH carbon measurements, Aerosol Sci. Technol., 34, 23-34, doi:
534 10.1080/02786820119073, 2001.
535 Chow, J.C., Watson, J.G., Chen, L.W.A., Arnott, W.P., Moosmuller, H., and Fung, K.:
536 Equivalence of elemental carbon by thermal/optical reflectance and transmittance
537 with different temperature protocols, Environ. Sci. Technol., 38, 4414-4422, doi:
538 10.1021/es034936u, 2004.
539 Chuang, C.C., Penner, J.E., Prospero, J.M., Grant, K.E., Rau, G.H., and Kawamoto, K.:
540 Cloud susceptibility and the first aerosol indirect forcing: Sensitivity to black
541 carbon and aerosol concentrations, J. Geophys. Res.-Atmos., 107, doi:
542 10.1029/2000JD000215, 2002.
543 Chylek, P., Srivastava, V., Cahenzli, L., Pinnick, R.G., Dod, R.L., Novakov, T., Cook, T.L.,
544 and Hinds, B.D.: Aerosol and Graphitic Carbon Content of Snow, J. Geophys. Res.-
545 Atmos., 92, 9801-9809, doi: 10.1029/JD092iD08p09801, 1987.
546 Clarke, A.D., Noone, K.J., Heintzenberg, J., Warren, S.G., and Covert, D.S.: Aerosol Light-
547 Absorption Measurement Techniques - Analysis and Intercomparisons, Atmos.
548 Environ., 21, 1455-1465, doi: 10.1016/0004-6981(67)90093-5, 1967.
549 Cong, Z., Kang, S., Kawamura, K., Liu, B., Wan, X., Wang, Z., Gao, S., and Fu, P.:
550 Carbonaceous aerosols on the south edge of the Tibetan Plateau: concentrations,

seasonality and sources, Atmos. Chem. Phys., 15, 1573-1584, doi: 10.5194/acp-15-1573-2015, 2015.

Cross, E.S., Onasch, T.B., Ahern, A., Wrobel, W., Slowik, J.G., Olfert, J., Lack, D.A., Massoli, P., Cappa, C.D., Schwarz, J.P., Spackman, J.R., Fahey, D.W., Sedlacek, A., Trimborn, A., Jayne, J.T., Freedman, A.,Williams, L.R., Ng, N.L., Mazzoleni, C., Dubey, M., Brem, B., Kok, G., Subramanian, R., Freitag, S., Clarke, A., Thornhill, D., Marr, L.C., Kolb, C.E., Worsnop, D.R., and Davidovits, P.: Soot Particle Studies-Instrument Inter-Comparison-Project Overview, Aerosol Sci. Technol., 44, 592–611, 2010.

Dang, C. and Hegg, D.A.: Quantifying light absorption by organic carbon in Western North American snow by serial chemical extractions, J. Geophys. Res.-Atmos., 119, 10247-10261, doi: 10.1002/2014JD022156, 2014.

Doherty, S.J., Warren, S.G., Grenfell, T.C., Clarke, A.D., and Brandt, R.E.: Light-absorbing impurities in Arctic snow, Atmos. Chem. Phys., 10, 11647-11680, doi: 10.5194/acp-10-11647-2010, 2010.

Doherty, S.J., Dang, C., Hegg, D.A., Zhang, R.D., and Warren, S.G.: Black carbon and other light-absorbing particles in snow of central North America, J. Geophys. Res.-Atmos., 119, 12807-12831, doi: 10.1002/2014JD022350, 2014.

Fischer K.: Bestimmung der Absorption von sichtbarer Strahlung durch Aerosolpartikeln, Contr. Atmos. Phys., 43, 244-254, 1970.

Flanner, M.G., Liu, X., Zhou, C., Penner, J.E., and Jiao, C.: Enhanced solar energy absorption by internally-mixed black carbon in snow grains, Atmos. Chem. Phys., 12, 4699-4721, doi: 10.5194/acp-12-4699-2012, 2012.

Forsstrom, S., Isaksson, E., Skeie, R.B., Strom, J., Pedersen, C.A., Hudson, S.R., Berntsen, T.K., Lihavainen, H., Godtliebsen, and F., Gerland, S.: Elemental carbon measurements in European Arctic snow packs, J. Geophys. Res.-Atmos., 118, 13614-13627, doi: 10.1002/2013JD019886, 2013.

Gillies, J. A., Gertler, A.W., Sagebiel, J.C., Dippel, W.A.: On-road particulate matter (PM2.5 and PM10) emissions in the Sepulveda Tunnel, Los Angeles, California. Environ. Sci. Technol., 35, 1054-1063, 2001.

580 Gray, H. A., Cass, G. R., Huntzicker, J. J., Heyerdahl, E.K., Rau, J.A.: Characteristics of
581 Atmospheric Organic and Elemental Carbon Particle Concentrations in Los-Angeles.
582 Environ. Sci. Technol., 20, 580-589, doi: 10.1021/Es00148a006, 1986.
583 Grenfell, T.C., Doherty, S.J., Clarke, A.D., and Warren, S.G.: Light absorption from
584 particulate impurities in snow and ice determined by spectrophotometric analysis
585 of filters, Appl. Opt., 50, 2037-2048, doi: 10.1364/AO.50.002037, 2011.
586 Hadley, O.L., Corrigan, C.E., Kirchstetter, T.W., Cliff, S.S., and Ramanathan, V.:
587 Measured black carbon deposition on the Sierra Nevada snow pack and implication
588 for snow pack retreat, Atmos. Chem. Phys., 10, 7505-7513, doi: 10.5194/acp-10-
589 7505-2010, 2010.
590 Hadley, O.L. and Kirchstetter, T.W.: Black-carbon reduction of snow albedo, Nat. Clim.
591 Chang., 2, 437-440, doi: 10.1038/NCLIMATE1433, 2012.
592 Han, Y. M., Han, Z. W., Cao, J. J., Chow, J.C., Watson, J.G., An, Z.S., Liu, S.X., Zhang, R.J.:
593 Distribution and origin of carbonaceous aerosol over a rural high-mountain lake
594 area, Northern China and its transport significance. Atmos. Environ., 42, 2405-2414,
595 doi: 10.1016/j.atmosenv.2007.12.020, 2008.
596 Hansen, A. D. A., Rosen, H., and Novakov, T.: The aethalometer — An instrument for
597 the real-time measurement of optical absorption by aerosol particles, Sci. Total
598 Environ., 36, 191-196, doi: 10.1016/0048-9697(84)90265-1, 1984.
599 Hansen, J., Sato, M., Ruedy, R., Nazarenko, L., Lacis, A., Schmidt, G.A., Russell, G., Aleinov,
600 I., Bauer, M., Bauer, S., Bell, N., Cairns, B., Canuto, V., Chandler, M., Cheng, Y., Del
601 Genio, A., Faluvegi, G., Fleming, E., Friend, A., Hall, T., Jackman, C., Kelley, M., Kiang,
602 N., Koch, D., Lean, J., Lerner, J., Lo, K., Menon, S., Miller, R., Minnis, P., Novakov, T.,
603 Oinas, V., Perlwitz, J., Perlwitz, J., Rind, D., Romanou, A., Shindell, D., Stone, P., Sun,
604 S., Tausnev, N., Thresher, D., Wielicki, B., Wong, T., Yao, M., and Zhang, S.: Efficacy of
605 climate forcings, J. Geophys. Res.-Atmos., 110, doi: 10.1029/2005JD005776, 2005.
606 Heintzenberg, J.: Fine particles in the global troposphere A review, Tellus B., 41, 149-
607 160, doi: 10.1111/j.1600-0889.1989.tb00132.x, 1989.

608 Hitzenberger, R.: Absorption-Measurements with an Integrating Plate Photometer
609 Calibration and Error Analysis, Aerosol Sci. Technol., 18, 70-84, doi:
610 10.1080/02786829308959585, 1993.
611 Horvath, H.: Comparison of Measurements of Aerosol Optical-Absorption by Filter
612 Collection and a Transmissometric Method, Atmos. Environ., 27, 319-325, doi:
613 10.1016/0960-1686(93)90105-8, 1993a.
614 Horvath, H.: Atmospheric Light-Absorption - a Review, Atmos. Environ., 27, 293-317,
615 doi: 10.1016/0960-1686(93)90104-7, 1993b.
616 Huang, J.P., Fu, Q.A., Zhang, W., Wang, X., Zhang, R.D., Ye, H., and Warren, S.G.: Dust and
617 Black Carbon in Seasonal Snow across Northern China, Bull. Amer. Meteor. Soc., 92,
618 175-181, doi: 10.1175/2010BAMS3064.1, 2011.
619 IPCC. 2013. Climate Change 2013: The Physical Science Basis[M]. Stocker, T. F., D . Qin,
620 G. K. Plattner, et al., Cambridge, United Kingdom and New York, NY, USA.
621 Ivleva, N. P., McKeon, U., Niessner, R., and Pöschl, U.: Raman microspectroscopic
622 analysis of size-resolved atmospheric aerosol particle samples collected with an
623 ELPI: Soot, humic-like substances, and inorganic compounds, Aerosol Sci. Technol.,
624 41, 655–671, doi:10.1080/02786820701376391, 2007.
625 Jacobson, M.Z.: Strong radiative heating due to the mixing state of black carbon in
626 atmospheric aerosols, Nature 409, 695-697, doi: 10.1038/35055518, 2001a.
627 Jacobson, M.Z.: Global direct radiative forcing due to multicomponent anthropogenic
628 and natural aerosols, J. Geophys. Res.-Atmos., 106, 1551-1568, doi:
629 10.1029/2000JD900514, 2001b.
630 Jenk, T.M., Szidat, S., Schwikowski, M., Gaggeler, H.W., Brutsch, S., Wacker, L., Synal,
631 H.A., and Saurer, M.: Radiocarbon analysis in an Alpine ice core: record of
632 anthropogenic and biogenic contributions to carbonaceous aerosols in the past
633 (1650-1940), Atmos. Chem. Phys., 6, 5381-5390, doi: 10.5194/acp-6-5381-2006,
634 2006.
635 Jimenez, J. L., Canagaratna, M. R., Donahue, N. M., Prevot, A.S.H., Zhang, Q., Kroll, J.H.,
636 DeCarlo, P.F., Allan, J.D., Coe, H., Ng, N.L., Aiken, A.C., Docherty, K.S., Ulbrich, I.M.,
637 Grieshop, A.P., Robinson, A.L., Duplissy, J., Smith, J.D., Wilson, K.R., Lanz, V.A.,

638 Hueglin, C., Sun, Y.L., Tian, J., Laaksonen, A., Raatikainen, T., Rautiainen, J.,
639 Vaattovaara, P., Ehn, M., Kulmala, M., Tomlinson, J.M., Collins, D.R., Cubison, M.J.,
640 Dunlea, E.J., Huffman, J.A., Onasch, T.B., Alfarra, M.R., Williams, P.I., Bower, K., Kondo,
641 Y., Schneider, J., Drewnick, F., Borrmann, S., Weimer, S., Demerjian, K., Salcedo, D.,
642 Cottrell, L., Griffin, R., Takami, A., Miyoshi, T., Hatakeyama, S., Shimono, A., Sun, J.Y.,
643 Zhang, Y.M., Dzepina, K., Kimmel, J.R., Sueper, D., Jayne, J.T., Herndon, S.C., Trimborn,
644 A.M., Williams, L.R., Wood, E.C., Middlebrook, A.M., Kolb, C.E., Baltensperger, U.,
645 Worsnop, D.R.: Evolution of organic aerosols in the atmosphere, Science, 326,
646 1525–1529, 2009.
647 Koch, D., Schulz, M., Kinne, S., McNaughton, C., Spackman, J.R., Balkanski, Y., Bauer, S.,
648 Berntsen, T., Bond, T.C., Boucher, O., Chin, M., Clarke, A., De Luca, N., Dentener, F.,
649 Diehl, T., Dubovik, O., Easter, R., Fahey, D.W., Feichter, J., Fillmore, D., Freitag, S.,
650 Ghan, S., Ginoux, P., Gong, S., Horowitz, L., Iversen, T., Kirkevag, A., Klimont, Z.,
651 Kondo, Y., Krol, M., Liu, X., Miller, R., Montanaro, V., Moteki, N., Myhre, G., Penner,
652 J.E., Perlwitz, J., Pitari, G., Reddy, S., Sahu, L., Sakamoto, H., Schuster, G., Schwarz, J.P.,
653 Seland, O., Stier, P., Takegawa, N., Takemura, T., Textor, C., van Aardenne, J.A., and
654 Zhao, Y.: Evaluation of black carbon estimations in global aerosol models, Atmos.
655 Chem. Phys., 9, 9001-9026, doi: 10.5194/acp-9-9001-2009, 2009.
656 Legrand, M., Preunkert, S., Schock, M., Cerqueira, M., Kasper-Giebl, A., Afonso, J., Pio,
657 C., Gelencser, A., and Dombrowski-Etchevers, I.: Major 20th century changes of
658 carbonaceous aerosol components (EC, WinOC, DOC, HULIS, carboxylic acids, and
659 cellulose) derived from Alpine ice cores, J. Geophys. Res.-Atmos., 112, doi:
660 10.1029/2006JD008080, 2007.
661 Li, W., Shao, L., Zhang, D., Ro, C.-U., Hu, M., Bi, X., Geng, H., Matsuki, A., Niu, H., and Chen,
662 J.: A review of single aerosol particle studies in the atmosphere of East Asia:
663 morphology, mixing state, source, and heterogeneous reactions, J. Clean Prod., 112,
664 1330-1349, https://doi.org/10.1016/j.jclepro.2015.04.050, 2016.
665 Lim, S., Fain, X., Zanatta, M., Cozic, J., Jaffrezo, J.L., Ginot, P., and Laj, P.: Refractory black
666 carbon mass concentrations in snow and ice: method evaluation and inter-

667 comparison with elemental carbon measurement, Atmos. Meas. Tech., 7, 3307-
668 3324, doi: 10.5194/amt-7-3307-2014, 2014.
669 McMeeking, G.R., Morgan, W.T., Flynn, M., Highwood, E.J., Turnbull, K., Haywood, J.,
670 and Coe, H.: Black carbon aerosol mixing state, organic aerosols and aerosol optical
671 properties over the United Kingdom, Atmos. Chem. Phys., 11, 9037-9052, doi:
672 10.5194/acp-11-9037-2011, 2011.
673 Menon, S., Hansen, J., Nazarenko, L., Luo, Y.F.: Climate effects of black carbon aerosols
674 in China and India, Science 297, 2250-2253, doi: 10.1126/science.1075159, 2002.
675 Ming, J., Cachier, H., Xiao, C., Qin, D., Kang, S., Hou, S., and Xu, J.: Black carbon record
676 based on a shallow Himalayan ice core and its climatic implications, Atmos. Chem.
677 Phys., 8, 1343-1352, doi: 10.5194/acp-8-1343-2008, 2008.
678 Ming, J., Xiao, C.D., Cachier, H., Qin, D.H., Qin, X., Li, Z.Q., and Pu, J.C.: Black Carbon (BC)
679 in the snow of glaciers in west China and its potential effects on albedos, Atmos.
680 Res., 92, 114-123, doi: 10.1016/j.atmosres.2008.09.007, 2009.
681 Ming, J., Xiao, C.D., Sun, J.Y., Kang, S.C., and Bonasoni, P.: Carbonaceous particles in the
682 atmosphere and precipitation of the Nam Co region, central Tibet, J. Environ. Sci.,
683 22, 1748-1756, doi: 10.1016/S1001-0742(09)60315-6, 2010.
684 Moosmuller, H., Chakrabarty, R.K., and Arnott, W.P.: Aerosol light absorption and its
685 measurement: A review, J. Quant. Spectrosc. Ra., 110, 844-878, doi:
686 10.1016/j.jqsrt.2009.02.035, 2009.
687 Moteki, N., Kondo, Y., Takegawa, N., and Nakamura, S.-i.: Directional dependence of
688 thermal emission from nonspherical carbon particles, J. Aerosol Sci., 40, 790-801,
689 doi: 10.1016/j.jaerosci.2009.05.003, 2009.
690 Murphy, D. M., Cziczo, D. J., Froyd, K. D., Hudson, P. K., Matthew, B. M., Middlebrook, A.
691 M., Peltier, R. E., Sullivan, A., Thomson, D. S., Weber, R. J.: Single-particle mass
692 spectrometry of tropospheric aerosol particles. J. Geophys. Res., 111, D23S32,
693 doi:10.1029/2006JD007340, , 2006.
694 Ogren, J. A. and Charlson, R. J.: Elemental carbon in the atmosphere– cycle and lifetime,
695 Tellus, 35B, 241–254, 1983.

696 Painter, T.H., Seidel, F.C., Bryant, A.C., Skiles, S.M., and Rittger, K.: Imaging
697 spectroscopy of albedo and radiative forcing by light-absorbing impurities in
698 mountain snow, J. Geophys. Res.-Atmos., 118, 9511-9523, doi: 10.1002/jgrd.50520,
699 2013.
700 Pan, Y.P., Wang, Y.S., Xin, J.Y., Tang, G.Q., Song, T., Wang, Y.H., Li, X.R., and Wu, F.K.:
701 Study on dissolved organic carbon in precipitation in Northern China, Atmos.
702 Environ., 44, 2350-2357, doi: 10.1016/j.atmosenv.2010.03.033, 2010.
703 Pavese, G., Calvello, M., and Esposito, F.: Black Carbon and Organic Components in the
704 Atmosphere of Southern Italy: Comparing Emissions from Different Sources and
705 Production Processes of Carbonaceous Particles, Aerosol Air Qual. Res., 12, 1146-
706 1156, doi: 10.4209/aaqr.2011.12.0236, 2012.
707 Pedersen, C.A., Gallet, J.C., Strom, J., Gerland, S., Hudson, S.R., Forsstrom, S., Isaksson,
708 E., and Berntsen, T. K.: In situ observations of black carbon in snow and the
709 corresponding spectral surface albedo reduction, J. Geophys. Res.-Atmos., 120,
710 1476-1489, doi: 10.1002/2014jd022407, 2015.
711 Petzold, A., Kopp, C., and Niessner, R.: The dependence of the specific attenuation
712 cross-section on black carbon mass fraction and particle size, Atmos. Environ., 31,
713 661-672, doi: 10.1016/S1352-2310(96)00245-2, 1997.
714 Petzold, A., Ogren, J. A., Fiebig, M., Laj, P., Li, S.-M., Baltensperger, U., Holzer-Popp, T.,
715 Kinne, S., Pappalardo, G., Sugimoto, N., Wehrli, C., Wiedensohler, A., and Zhang, X.-
716 Y.: Recommendations for reporting "black carbon" measurements, Atmos. Chem.
717 Phys., 13, 8365-8379, https://doi.org/10.5194/acp-13-8365-2013, 2013.
718 Qian, Y., Wang, H., Zhang, R., Flanner, M.G., and Rasch, P.J.: A sensitivity study on
719 modeling black carbon in snow and its radiative forcing over the Arctic and
720 Northern China, Environ. Res. Lett., 9, 064001, doi: 10.1088/1748-
721 9326/9/6/064001, 2014.
722 Quinn, P. K. and Bates, T. S.: North American, Asian, and Indian haze: Similar regional
723 impacts on climate? Geophys. Res. Lett., 30, 1555, doi:10.1029/2003GL016934,
724 2003.

725 Ramanathan, V., and Carmichael, G.: Global and regional climate changes due to black
726 carbon, Nat. Geosci. , 1, 221-227, Doi 10.1038/Ngeo156, 2008.
727 Rosenfeld, D., Lohmann, U., Raga, G.B., O'Dowd, C.D., Kulmala, M., Fuzzi, S., Reissell, A.,
728 and Andreae, M.O.: Flood or drought: How do aerosols affect precipitation? Science
729 321, 1309-1313, doi: 10.1126/science.1160606, 2008.
730 Schmid, H., Laskus, L., Abraham, H.J., Baltensperger, U., Lavanchy, V., Bizjak, M., Burba,
731 P., Cachier, H., Crow, D., Chow, J., Gnauk, T., Even, A., ten Brink, H.M., Giesen, K.P.,
732 Hitzenberger, R., Hueglin, C., Maenhaut, W., Pio, C., Carvalho, A., Putaud, J.P., Toom-
733 Sauntry, D., and Puxbaum, H.: Results of the "carbon conference" international
734 aerosol carbon round robin test stage I, Atmos. Environ., 35, 2111-2121, doi:
735 10.1016/S1352-2310(00)00493-3, 2001.
736 Schwarz, J.P., Doherty, S.J., Li, F., Ruggiero, S.T., Tanner, C.E., Perring, A.E., Gao, R.S.,
737 and Fahey, D.W.: Assessing Single Particle Soot Photometer and Integrating
738 Sphere/Integrating Sandwich Spectrophotometer measurement techniques for
739 quantifying black carbon concentration in snow, Atmos. Meas. Tech., 5, 2581-2592,
740 doi: 10.5194/amt-5-2581-2012, 2012.
741 Sharma, S., Brook, J.R., Cachier, H., Chow, J., Gaudenzi, A., and Lu, G.: Light absorption
742 and thermal measurements of black carbon in different regions of Canada, J.
743 Geophys. Res.-Atmos., 107, doi: 10.1029/2002JD002496, 2002.
744 Slater, J.F., Currie, L.A., Dibb, J.E., and Benner, B.A.: Distinguishing the relative
745 contribution of fossil fuel and biomass combustion aerosols deposited at Summit,
746 Greenland through isotopic and molecular characterization of insoluble carbon,
747 Atmos. Environ., 36, 4463-4477, doi: 10.1016/S1352-2310(02)00402-8, 2002.
748 Spencer, M.T., Shields, L.G., and Prather, K. A.: Simultaneous measurement of the
749 effective density and chemical composition of ambient aerosol particles, Environ.
750 Sci. Technol., 41, 1303–1309, doi:10.1021/es061425+, 2007.
751 Thevenon, F., Anselmetti, F.S., Bernasconi, S.M., and Schwikowski, M.: Mineral dust
752 and elemental black carbon records from an Alpine ice core (Colle Gnifetti glacier)
753 over the last millennium, J. Geophys. Res.-Atmos., 114, doi:
754 10.1029/2008JD011490, 2009.

Turpin, B. J., Cary, R. A., and Huntzicker, J. J.: An insitu,time-resolved analyzer for aerosol organic and elemental carbon. Aerosol Sci. Technol., 12, 161-171, doi: 10.1080/02786829008959336, 1990.

Turpin, B. J., and Huntzicker, J. J.: Secondary formation of organic aerosol in the Los Angeles Basin: A descriptive analysis of organic and elemental carbon concentrations. Atmos. Environ., 25A, 207-215, 1991.

von Schneidemesser, E., Schauer, J.J., Hagler, G.S.W., and Bergin, M.H.: Concentrations and sources of carbonaceous aerosol in the atmosphere of Summit, Greenland, Atmos. Environ., 43, 4155-4162, doi: 10.1016/j.atmosenv.2009.05.043, 2009.

Wang, M., Xu, B., Zhao, H., Cao, J., Joswiak, D., Wu, G., and Lin, S.: The Influence of Dust on Quantitative Measurements of Black Carbon in Ice and Snow when Using a Thermal Optical Method, Aerosol Sci. Technol., 46, 60-69, doi: 10.1080/02786826.2011.605815, 2012.

Wang, X., Doherty, S.J., and Huang, J.P.: Black carbon and other light-absorbing impurities in snow across Northern China, J. Geophys. Res.-Atmos., 118, 1471-1492, doi: 10.1029/2012JD018291, 2013.

Wang, X., Pu, W., Ren, Y., Zhang, X.L., Zhang, X.Y., Shi, J.S., Jin, H.C., Dai, M.K., Chen, Q.L.: Observations and model simulations of snow albedo reduction in seasonal snow due to insoluble light-absorbing particles during 2014 Chinese survey, Atmos. Chem. Phys., 17, 2279-2296, doi: 10.5194/acp-17-2279-2017, 2017.

Wang, R, Tao, S., Balkanski, Y., Ciais, P., Boucher, O., Liu, J.F., Piao, S.L., Shen, H.Z., Vuolo, M.R., Valari, M., Chen, H., Chen, Y.C., Cozic, A., Huang, Y., Li, B.A., Li, W., Shen, G.F., Wang, B., Zhang, Y.Y.: Exposure to ambient black carbon derived from a unique inventory and high-resolution model. Proc. Natl. Acad. Sci. USA., 111, 2459-2461, doi: 10.1073/pnas.1318763111, 2014.

Watson, J. G., and Chow, J. C.: Comparison and evaluation of in situ and filter carbon measurements at the Fresno Supersite, J. Geophys. Res.-Atmos., 107, doi:10.1029/2001jd000573, 2002.

783 Wolff, E.W. and Cachier, H.: Concentrations and seasonal cycle of black carbon in
784 aerosol at a coastal Antarctic station, J. Geophys. Res.-Atmos., 103, 11033-11041,
785 doi: 10.1029/97JD01363, 1998.
786 Xu, B.Q., Yao, T.D., Liu, X.Q., and Wang, N.L.: Elemental and organic carbon
787 measurements with a two-step heating-gas chromatography system in snow
788 samples from the Tibetan Plateau, Annals of Glaciology, Vol 43, 2006 43, 257-262,
789 doi: 10.3189/172756406781812122, 2006.
790 Xu, B.Q., Cao, J.J., Hansen, J., Yao, T.D., Joswia, D.R., Wang, N.L., Wu, G.J., Wang, M., Zhao,
791 H.B., Yang, W., Liu, X.Q., and He, J.Q.: Black soot and the survival of Tibetan glaciers,
792 Proc. Nat. Acad. Sci. U.S.A., 106, 22114-22118, doi: 10.1073/pnas.0910444106,
793 2009a.
794 Xu, B.Q., Wang, M., Joswiak, D.R., Cao, J.J., Yao, T.D., Wu, G.J., Yang, W., and Zhao, H.B.:
795 Deposition of anthropogenic aerosols in a southeastern Tibetan glacier, J. Geophys.
796 Res.-Atmos., 114, doi: 10.1029/2008JD011510, 2009b.
797 Xu, B.Q., Cao, J.J., Joswiak, D.R., Liu, X.Q., Zhao, H.B., and He, J.Q.: Post-depositional
798 enrichment of black soot in snow-pack and accelerated melting of Tibetan glaciers,
799 Environ. Res. Lett., 7, doi: 10.1088/1748-9326/7/1/014022, 2012.
800 Yang, H., and Yu, J.Z.: Uncertainties in charring correction in the analysis of elemental
801 and organic carbon in atmospheric particles by thermal/optical methods, Environ.
802 Sci. Technol., 36, 5199-5204, doi: 10.1021/es025672z , 2002.
803 Yasunari, T. J., Tan, Q., Lau, K. M., Bonasoni, P., Marinoni, A., Laj, P., Menegoz, M.,
804 Takemura, T., and Chin, M.: Estimated range of black carbon dry deposition and the
805 related snow albedo reduction over Himalayan glaciers during dry pre-monsoon
806 periods, Atmos. Environ., 78, 259-267, doi:10.1016/j.atmosenv.2012.03.031, 2013.
807 Yasunari, T. J., Koster, R. D., Lau, W. K. M., Kim, K.: Impact of snow darkening via dust,
808 black carbon, and organic carbon on boreal spring climate in the Earth system. J.
809 Geophys. Res.-Atmos., 120, 5485-5503, doi: 10.1002/2014jd022977, 2015.
810 Ye, H., Zhang, R.D., Shi, J.S., Huang, J.P., Warren, S.G., and Fu, Q.: Black carbon in
811 seasonal snow across northern Xinjiang in northwestern China, Environ. Res. Lett.,
812 7, doi: 10.1088/1748-9326/7/4/044002, 2012.

Zhang, R.J., Ho, K.F., Cao, J.J., Han, Z.W., Zhang, M.G., Cheng, Y., and Lee, S.C.: Organic carbon and elemental carbon associated with PM10 in Beijing during spring time, J. Hazard. Mater., 172, 970-977, doi: 10.1016/j.jhazmat.2009.07.087, 2009.

Zhao, C., Hu, Z., Qian, Y., Leung, L.R., Huang, J., Huang, M., Jin, J., Flanner, M.G., Zhang, R., Wang, H., Yan, H., Lu, Z., and Streets, D.G.: Simulating black carbon and dust and their radiative forcing in seasonal snow: a case study over North China with field campaign measurements, Atmos. Chem. Phys., 14, 11475-11491, doi: 10.5194/acp-14-11475-2014, 2014

Zhou, Y., Wang, X., Wu, X.Q., Cong, Z.Y., Wu, G.M., Ji, M.X.: Quantifying Light Absorption of Iron Oxides and Carbonaceous Aerosol in Seasonal Snow across Northern China, Atmosphere-Basel, 8, doi: 10.3390/atmos8040063, 2017.

Figure captions:

Figure 1 Sampling locations. Sites 90–102 are located in northeast China and were used for snow sample collection during Jan–Feb. 2014. Snow sampling site 103 is located in Lanzhou in northwest China, and was used for atmospheric sample collection during 5–25 August 2015. Sites are numbered according to Wang et al. (2013) and Ye et al. (2012).

Figure 2 Schematic diagram of the improved two-sphere integrating spectrophotometer.

Figure 3 Calibration curve for standard fullerene soot at a wavelength of 550 nm. The solid line is a best-fit curve for the filter measurements. S_0 and S are the detected signals for the blank and sample filters, respectively, and $-\ln(S/S_0)$ is the relative attenuation.

Figure 4 Comparison of the theoretical and measured BC mass determined by the TSI and two-step techniques in the laboratory. The solid and dot–dashed lines represent best-fit lines for the TSI and two-step techniques, respectively. The dashed line is a 1:1 line.

Figure 5 Mass loss of standard fullerene soot on 1.0-μm quartz fiber filters determined by refiltration using 0.4-μm Nuclepore filters.

Figure 6 Comparison of BC concentrations in snow samples over northeast China during January–February 2014 determined by the TSI and two-step thermal optical methods. A 1:1 line (dashed) and a linear regression fit passing through the origin (solid curve) are also shown.

Figure 7 As for Fig. 6, but for atmospheric samples collected at Lanzhou in northwest China during 5–25 August 2015.

Figure 8 Spatial distributions of light absorption at 550 nm due to BC and non-BC fractions in surface snow across northern China during January–February 2014.

847 Figure 9 Variations in 8-hour (a) BC concentration and (b) BC and non-BC light absorption measured

848 by TSI spectrophotometer at 550 nm at Lanzhou during 5–25 August 2015 (day: 9 am to 5 pm; night:

849 11 pm to 7 am).

850

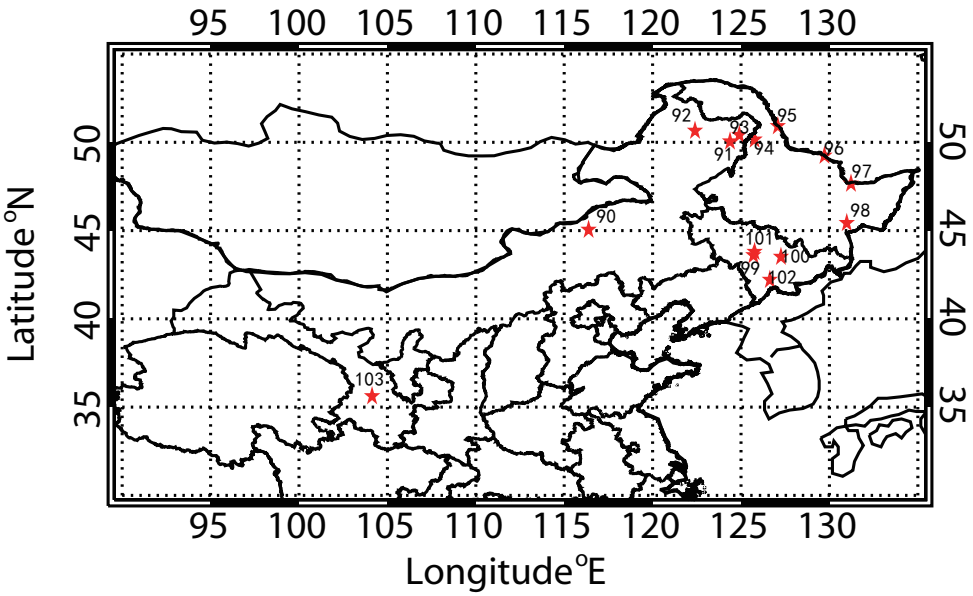

851

852 **Figure 1** Sampling locations. Sites 90–102 are located in northeast China and were used
853 for snow sample collection during Jan–Feb. 2014. Snow sampling site 103 is located in
854 Lanzhou in northwest China, and was used for atmospheric sample collection during 5–25
855 August 2015. Sites are numbered according to Wang et al. (2013) and Ye et al. (2012).

856

857 **Table 1** Series of 15 standard filters loaded with fullerene soot, and a comparison of BC
858 concentrations between theoretical calculations and the TSI/two-step thermal–optical
859 methods in the laboratory.
860

Filter	Standard BC Concentration ($\mu g/cm^2$)	Filter	Standard BC Concentration ($\mu g/cm^2$)	Filter	Calculated BC (μg)	TSI BC (μg)	Two-step BC (μg)
1	0.63	9	2.82	1	3.68	3.92	2.28
2	0.70	10	3.65	2	10.58	11.39	5.86
3	0.78	11	5.53	3	17.48	17.49	11.39
4	0.86	12	6.35	4	24.38	24.94	15.67
5	0.93	13	12.5	5	31.28	32.52	18.07
6	1.33	14	19.00	6	38.18	39.14	24.29
7	2.12	15	38.6	7	45.08	49.18	28.61
8	2.49	-	-	-	-	-	

861

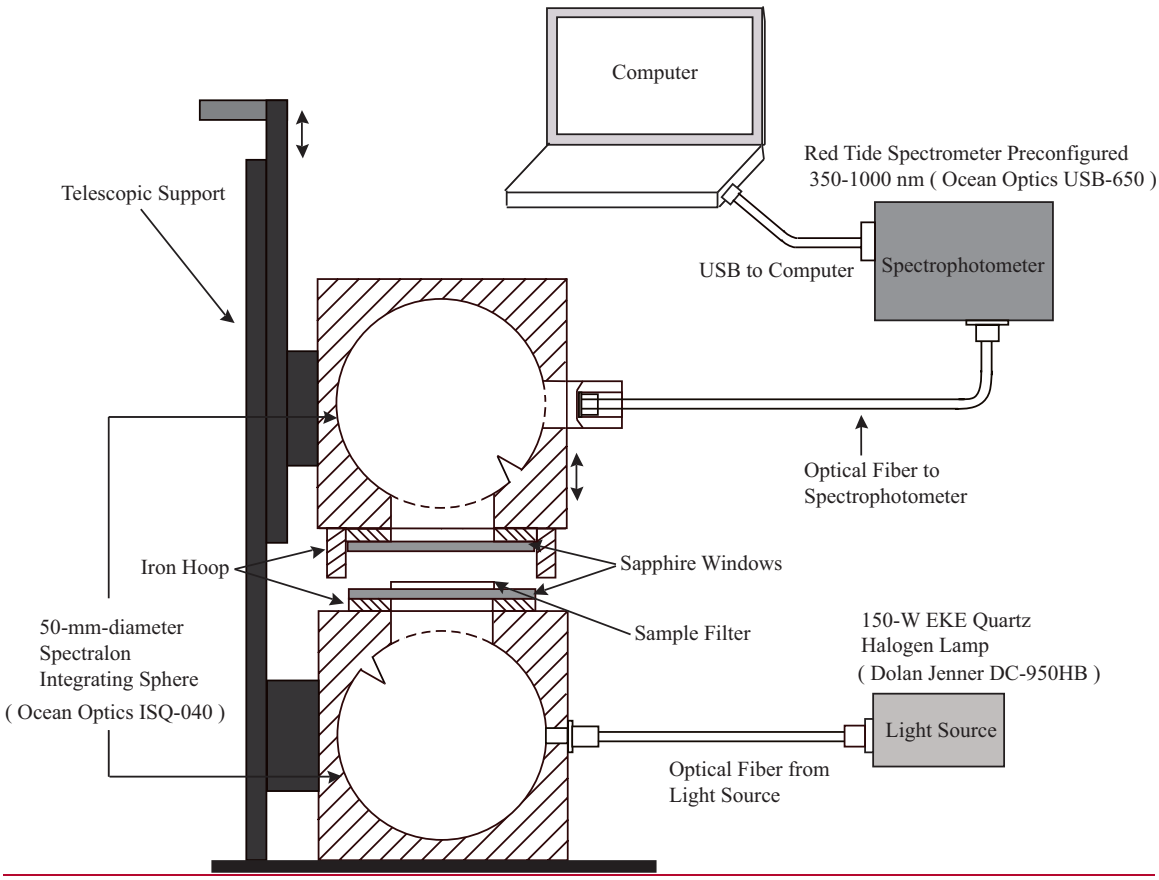

Figure 2 Schematic diagram of the improved two-sphere integrating spectrophotometer.

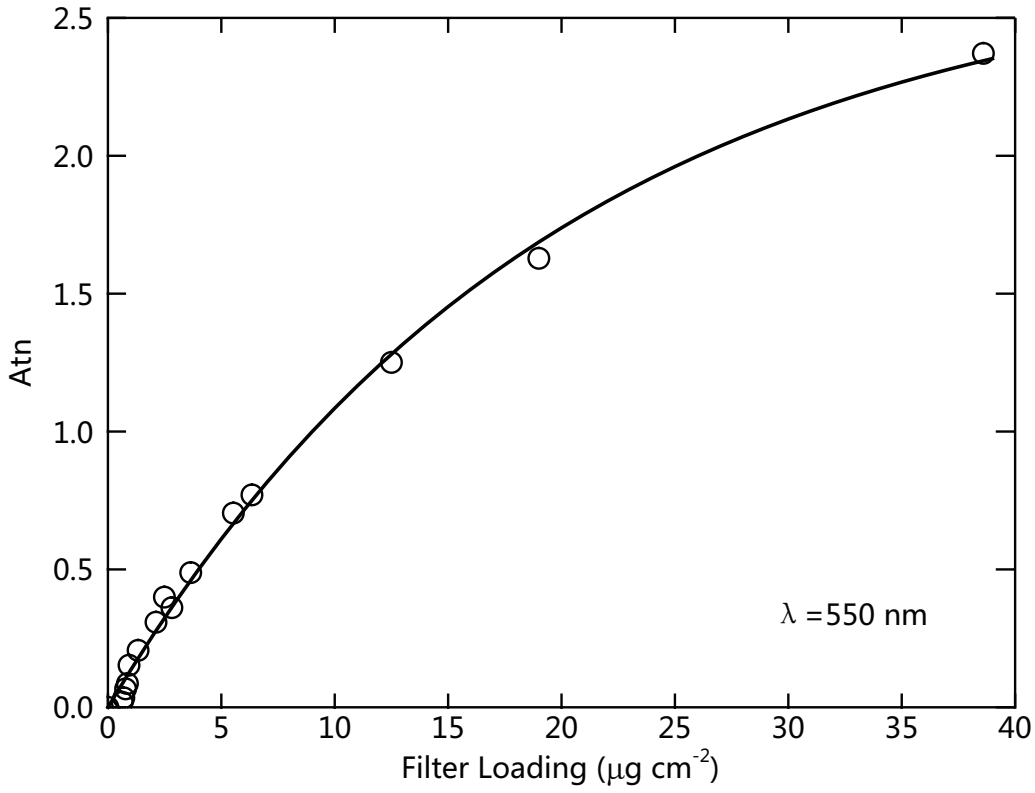

Figure 3 Calibration curve for standard fullerene soot at a wavelength of 550 nm. The solid line is a best-fit curve for the filter measurements. S_0 and S are the detected signals for the blank and sample filters, respectively, and $-\ln(S/S_0)$ is the relative attenuation.

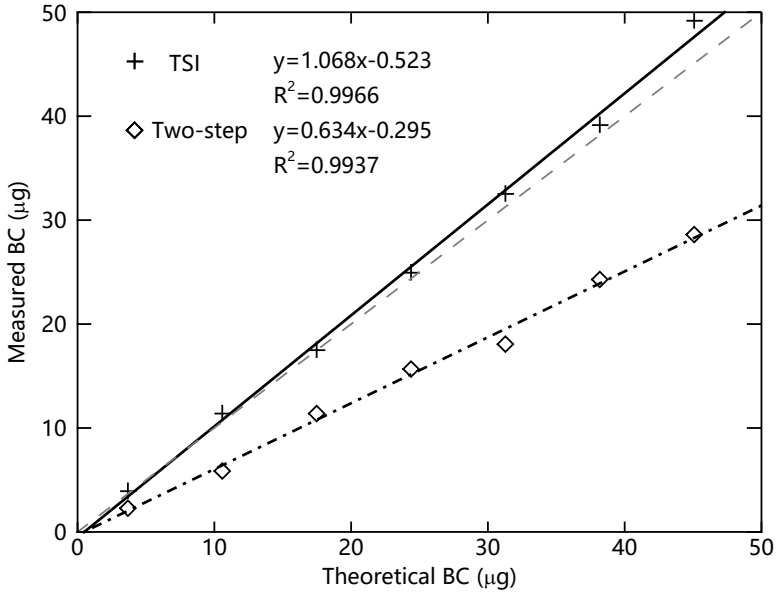

Figure 4 Comparison of the theoretical and measured BC mass determined by the TSI and two-step techniques in the laboratory. The solid and dot–dashed lines represent best-fit lines for the TSI and two-step techniques, respectively. The dashed line is a 1:1 line.

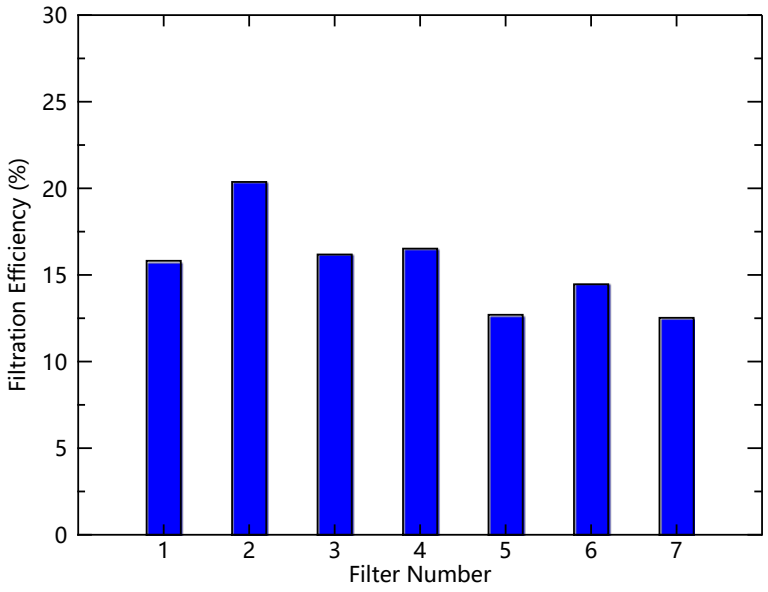

Figure 5 Mass loss of standard fullerene soot on 1.0-μm quartz fiber filters determined by refiltration using 0.4-μm Nuclepore filters.

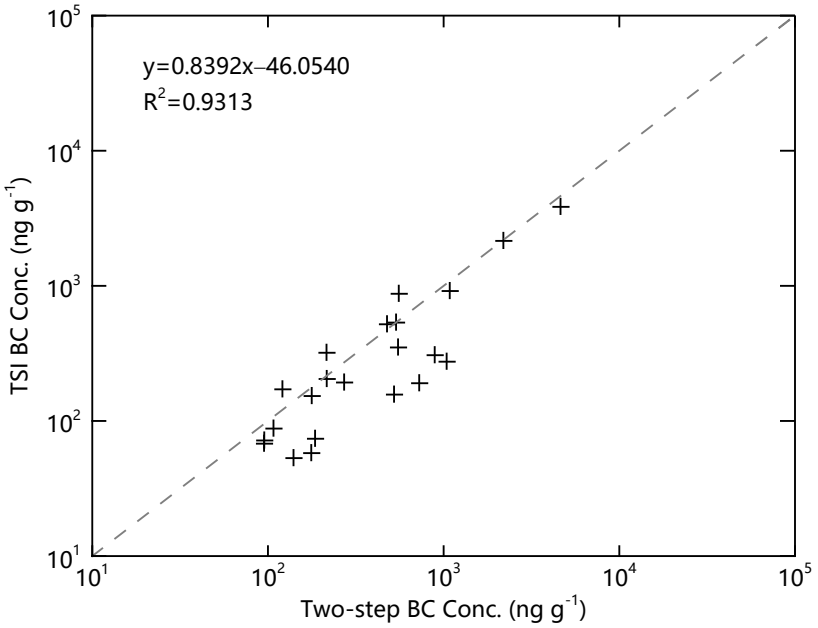

Figure 6 Comparison of BC concentrations in snow samples over northeast China during January–February 2014 determined by the TSI and two-step thermal optical methods. A 1:1 line (dashed) and a linear regression fit passing through the origin (solid curve) are also shown.

915

916

917

918

919

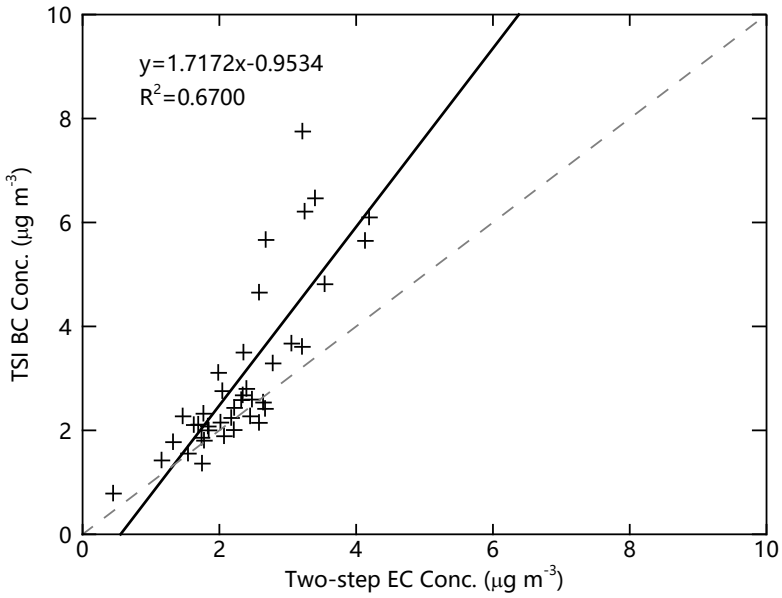

920

921 **Figure 7** As for Fig. 6, but for atmospheric samples collected at Lanzhou in northwest

922 China during 5–25 August 2015.

923

924 **Table 2** Statistics of BC and EC concentrations measured using the TSI and two-step
925 thermal–optical methods for snow samples during the experiments over northern China.
926
927

Site	Filter	TSI BC	Two-step EC
		ng g^{-1}	ng g^{-1}
90	Q-351L	349.95	550.19
91	Q-352L	171.46	120.87
	Q-352R	152.94	177.48
92	Q-354L	53.10	139.78
	Q-354R	57.82	176.41
93	Q-356L	71.71	95.27
	Q-356R	73.85	185.45
94	Q-358L	274.62	1040.20
95	Q-359L	87.84	107.51
	Q-359R	67.92	95.01
96	Q-363L	319.71	215.42
	Q-363R	192.60	271.42
97	Q-366L	204.47	216.04
	Q-366R	306.75	889.54
98	Q-369L	1605.95	130.36
	Q-369R	1321.69	6004.33
99	Q-376L	873.58	555.39
	Q-376R	534.70	536.11
100	Q-380R	519.47	476.14
101	Q-384R	3843.15	4626.72
102	Q-388L	915.59	1083.24
	Q-388R	2151.18	2187.90
103	Q-397L	156.76	522.07
	Q-397R	190.24	726.08

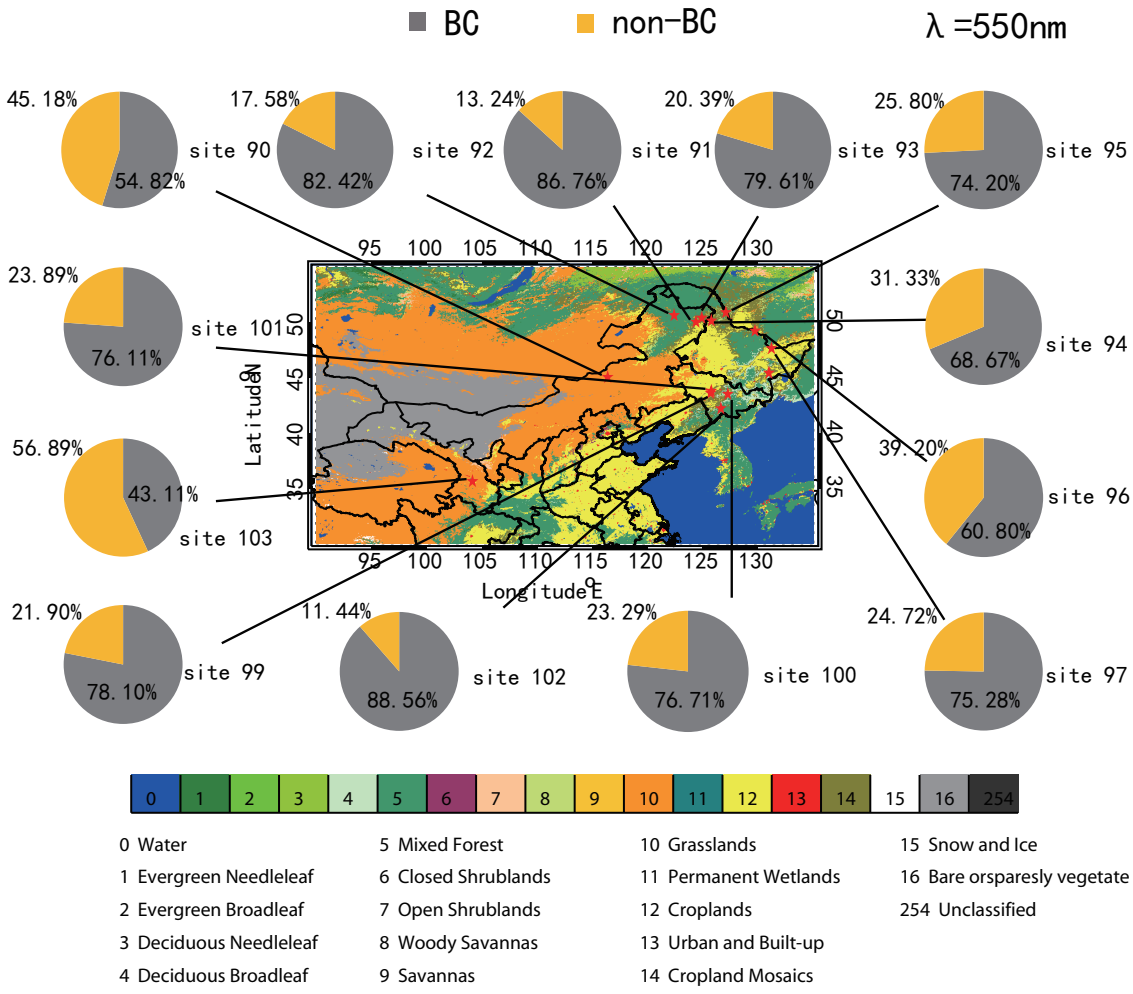

Figure 8 Spatial distributions of light absorption at 550 nm due to BC and non-BC fractions in surface snow across northern China during January–February 2014.

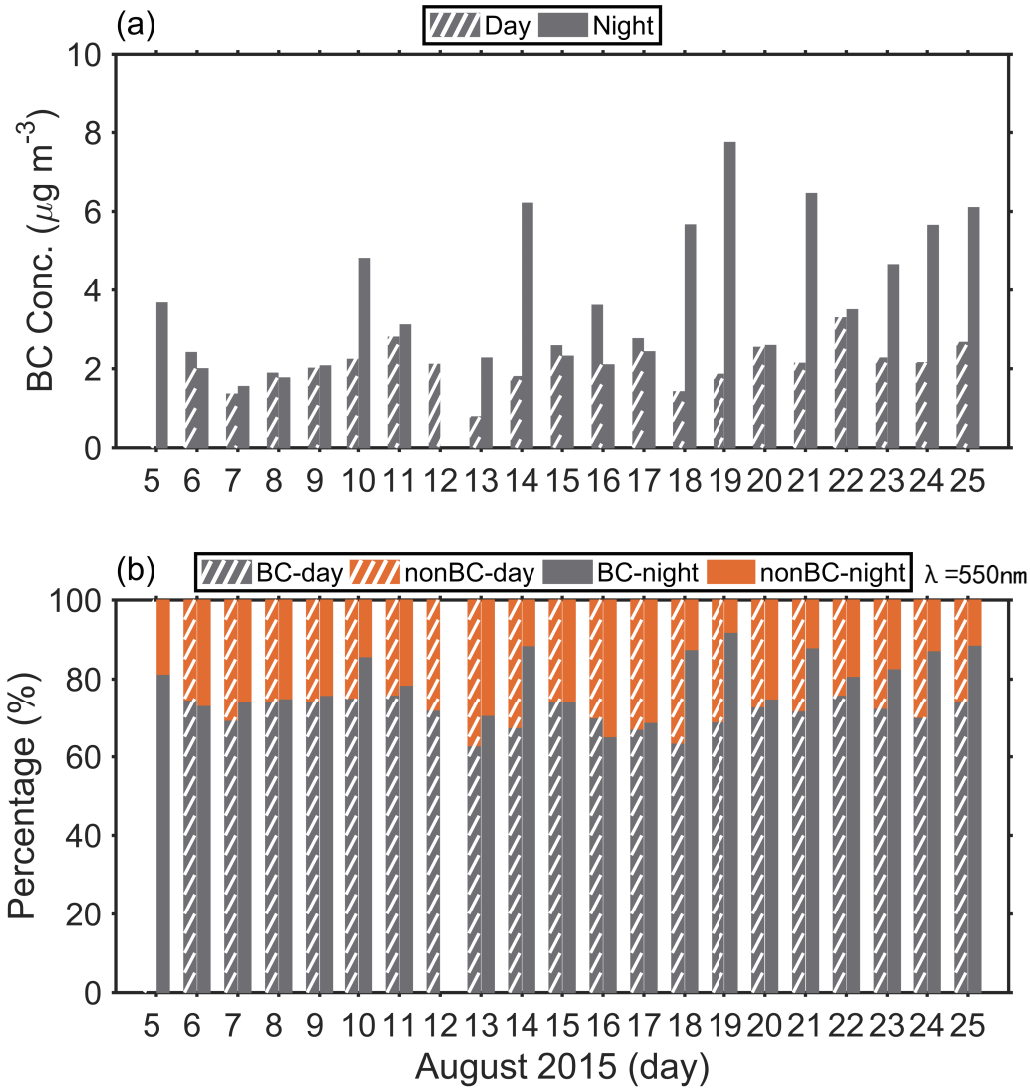

Figure 9 Variations in 8-hour **(a)** BC concentration and **(b)** BC and non-BC light absorption measured by TSI spectrophotometer at 550 nm at Lanzhou during 5–25 August 2015 (day: 9 am to 5 pm; night: 11 pm to 7 am).

939

940 **Table 3** Statistics of BC and EC concentrations in atmospheric samples measured using
941 the TSI and two-step thermal–optical methods.

Day			Night		
Date	TSI BC	Two-step EC	Date	TSI BC	Two-step EC
	μg m^{-3}	μg m^{-3}		μg m^{-3}	μg m^{-3}
2015.8.6	2.41	2.67	2015.8.5–8.6	3.67	3.05
2015.8.7	1.36	1.75	2015.8.6–8.7	2.00	1.84
2015.8.8	1.89	2.07	2015.8.7–8.8	1.55	1.54
2015.8.9	2.01	2.21	2015.8.8–8.9	1.77	1.32
2015.8.10	2.24	2.17	2015.8.9–8.10	2.07	1.83
2015.8.11	2.80	2.40	2015.8.10–8.11	4.81	3.54
2015.8.12	2.11	1.69	2015.8.11–8.12	3.11	1.98
2015.8.13	0.78	0.45	2015.8.13–8.14	2.27	1.46
2015.8.14	1.80	1.78	2015.8.14–8.15	6.21	3.25
2015.8.15	2.58	2.32	2015.8.15–8.16	2.32	1.77
2015.8.16	3.61	3.21	2015.8.16–8.17	2.10	1.63
2015.8.17	2.76	2.04	2015.8.17–8.18	2.43	2.22
2015.8.18	1.42	1.15	2015.8.18–8.19	5.66	2.68
2015.8.19	1.86	1.74	2015.8.19–8.20	7.75	3.21
2015.8.20	2.54	2.64	2015.8.20–8.21	2.59	2.48
2015.8.21	2.14	2.58	2015.8.21–8.22	6.46	3.40
2015.8.22	3.29	2.78	2015.8.22–8.23	3.50	2.35
2015.8.23	2.27	2.45	2015.8.23–8.24	4.65	2.58
2015.8.24	2.15	2.02	2015.8.24–8.25	5.65	4.13
2015.8.25	2.67	2.34	2015.8.25–8.26	6.10	4.19

942

943